

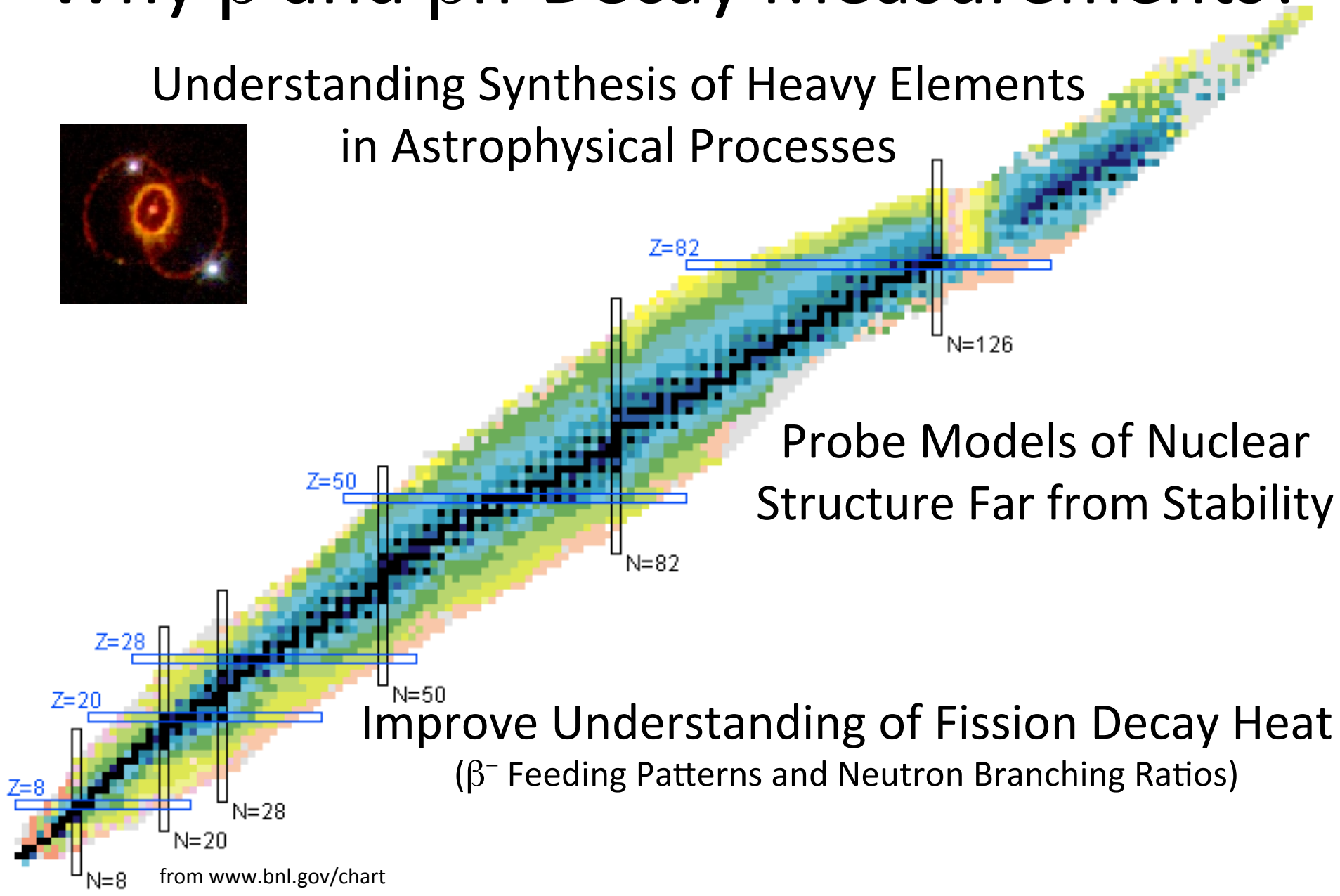
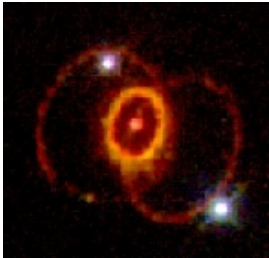
β -Decay Measurements of Neutron Rich Nuclei at the Holifield Radioactive Ion Beam Facility (HRIBF)

B. Charles Rasco
Louisiana State University

RIKEN June 12, 2012

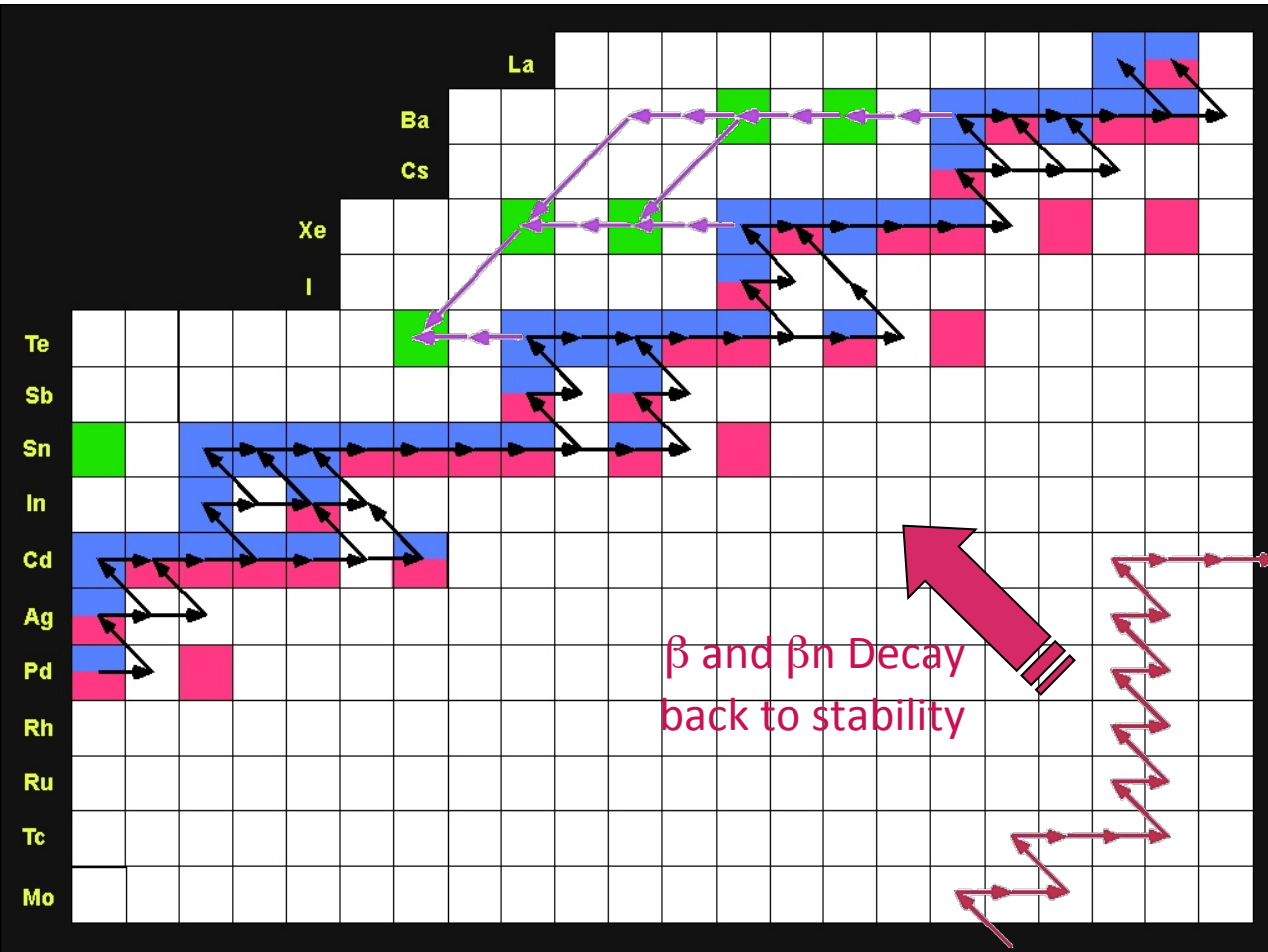
Why β and βn -Decay Measurements?

Understanding Synthesis of Heavy Elements
in Astrophysical Processes



Origin of the Elements

It is believed that there are three main types of processes that account for the observed elements in the universe



- s-Process

~80% of Isotopes

(n, γ) MACs Needed

Occurs in Asymptotic

Giant Branch (AGB) Stars

Branch Points Crucial

- r-Process

~70% of Isotopes

Far from Stability

Occurs Where?

- p-Process

~10% of Isotopes

Secondary Process

r-Process Example

Nucleosynthesis in the r-process

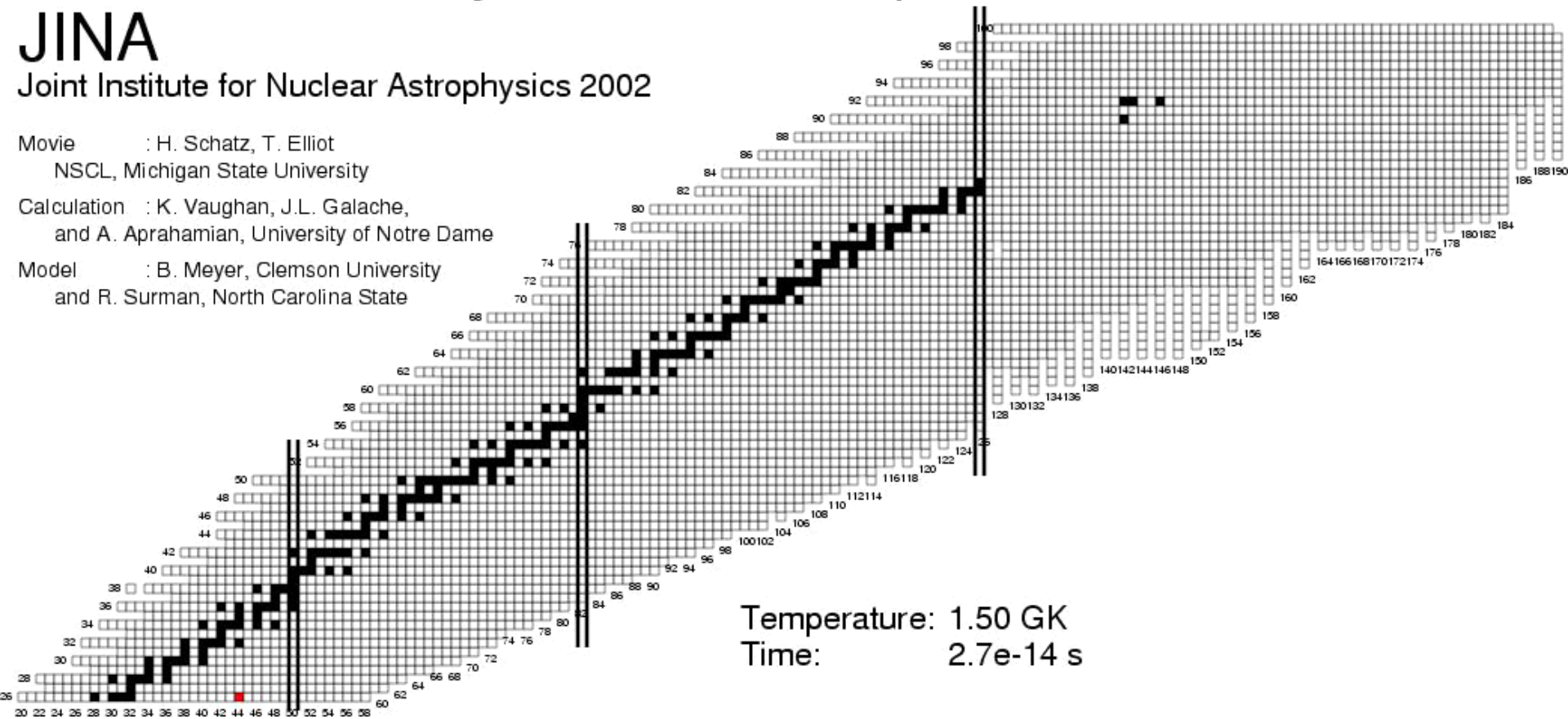
JINA

Joint Institute for Nuclear Astrophysics 2002

Movie : H. Schatz, T. Elliot
NSCL, Michigan State University

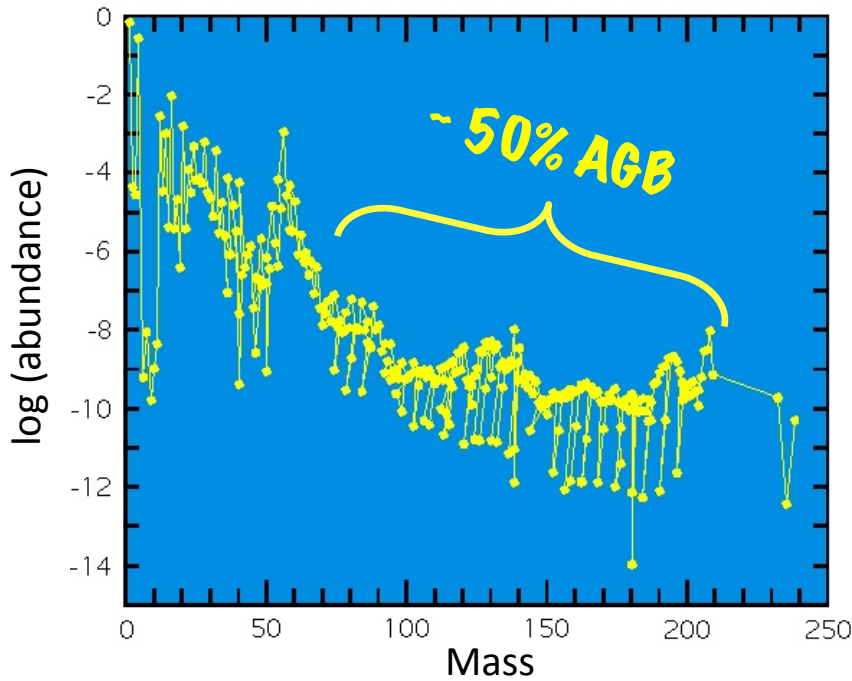
Calculation : K. Vaughan, J.L. Galache,
and A. Aprahamian, University of Notre Dame

Model : B. Meyer, Clemson University
and R. Surman, North Carolina State



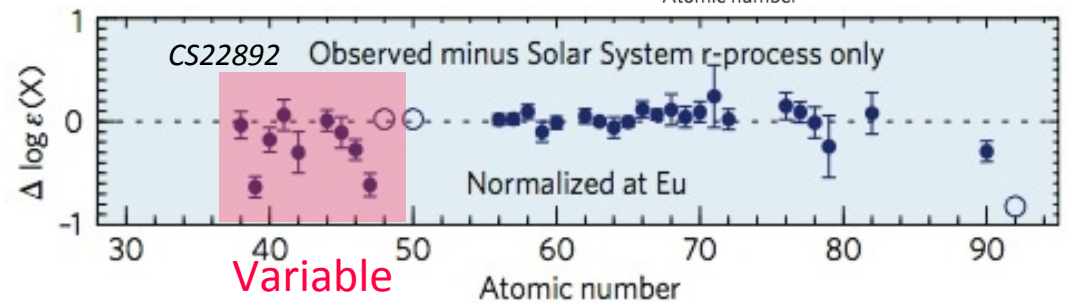
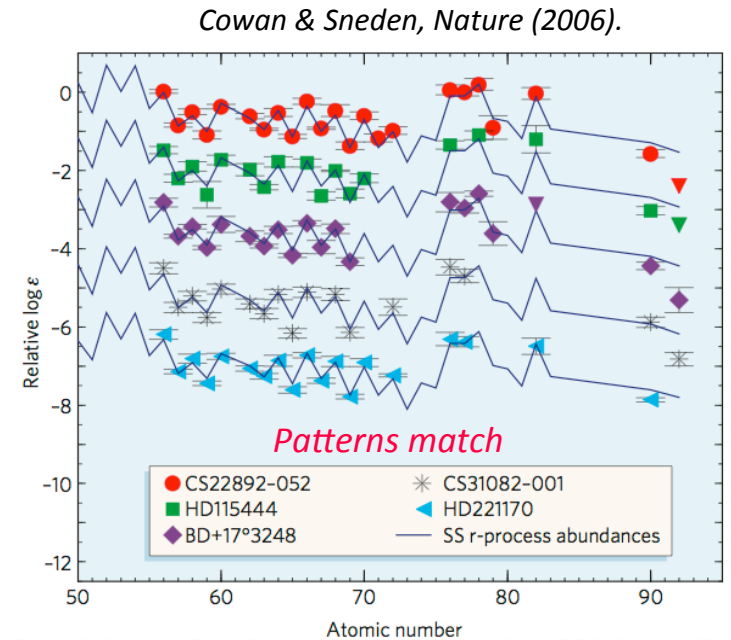
$T_{1/2}$, Nuclear Masses, and P_n (Neutron Emission Probability) Most Important to Measure
in Order to Predict Final Abundances of Elements Generated with the r-Process

Origin of the Elements



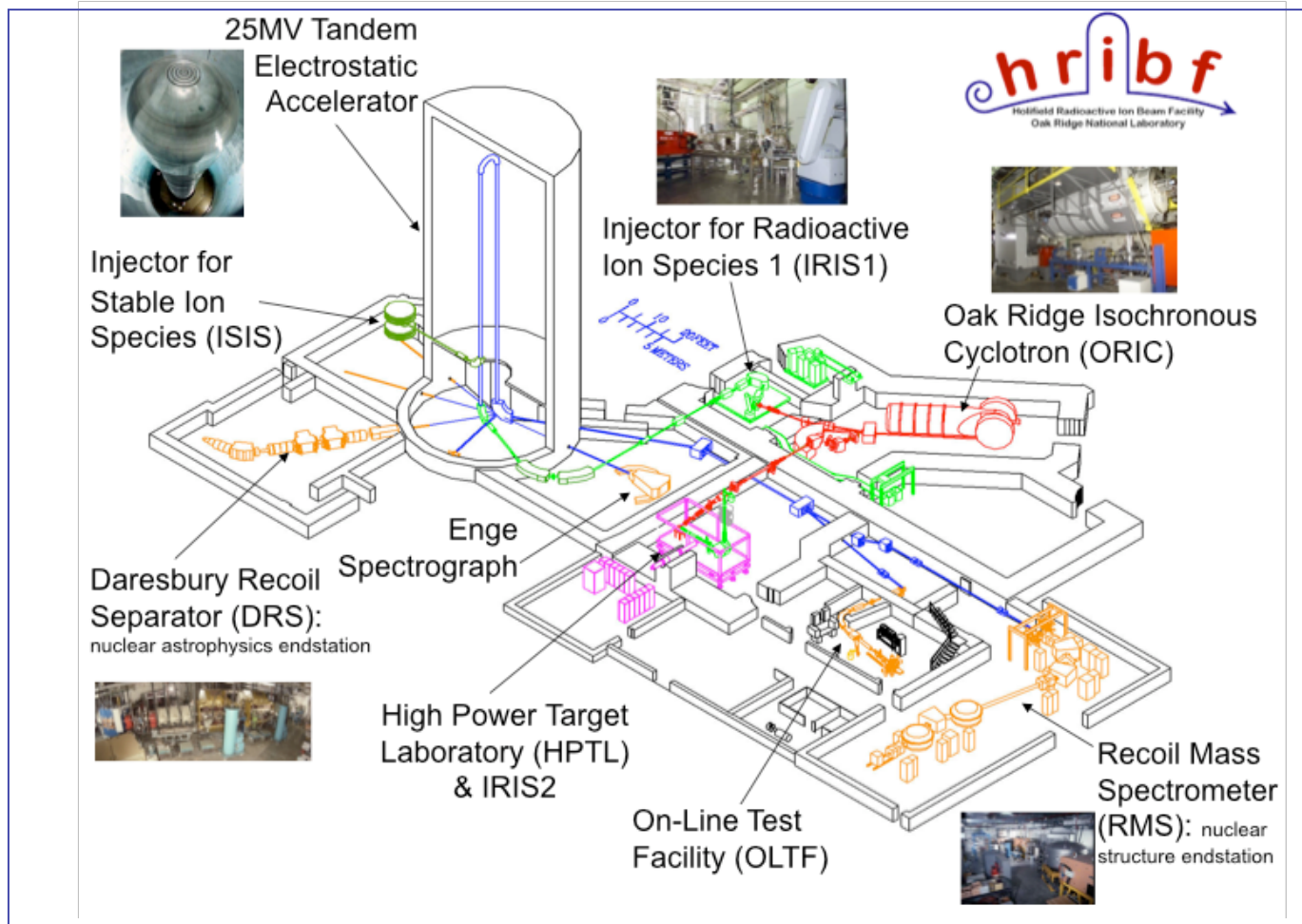
- Universal abundance pattern for heavy elements
 - r process
- Light elements vary
 - Other process?
 - Light Element Primary Process

- Changing paradigm
 - Spectra from old halo stars



Holifield Radioactive Ion Beam Facility(HRIBF) at Oak Ridge National Lab (ORNL)

Unfortunately the HRIBF has Ceased Operations
Further Studies at Argonne National Lab in the US and
TRIUMF in Canada are Possible



Useful Detectors Used in β Decay Studies

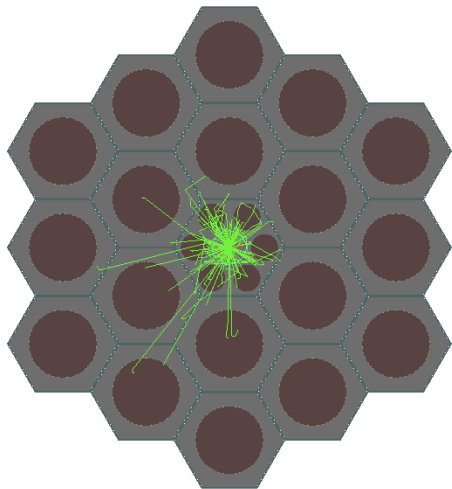
Gamma Detector Limitations: **Low Efficiency**, Poor Energy Resolution (NaI)

Neutron Detector Limitations: Low Efficiency, Poor Energy Resolution, γ Discrimination

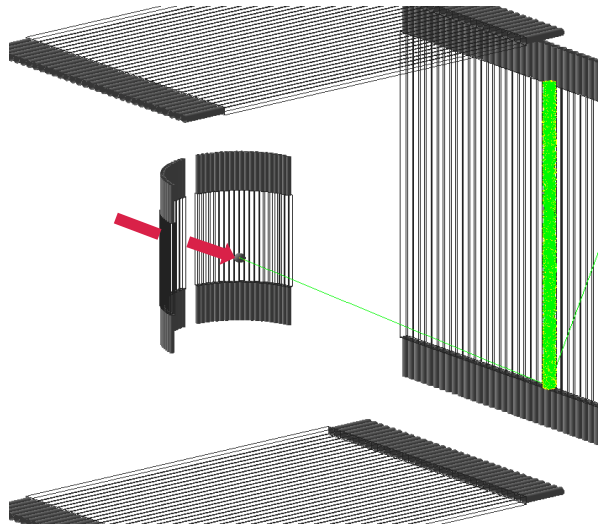
Electron Detector Limitations: Energy Threshold, γ Discrimination

Three New Detectors at ORNL Address these Detector Limitations

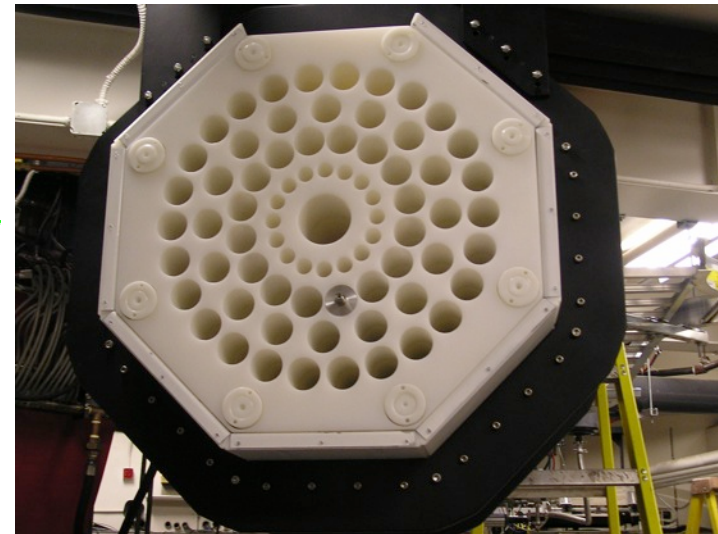
MTAS



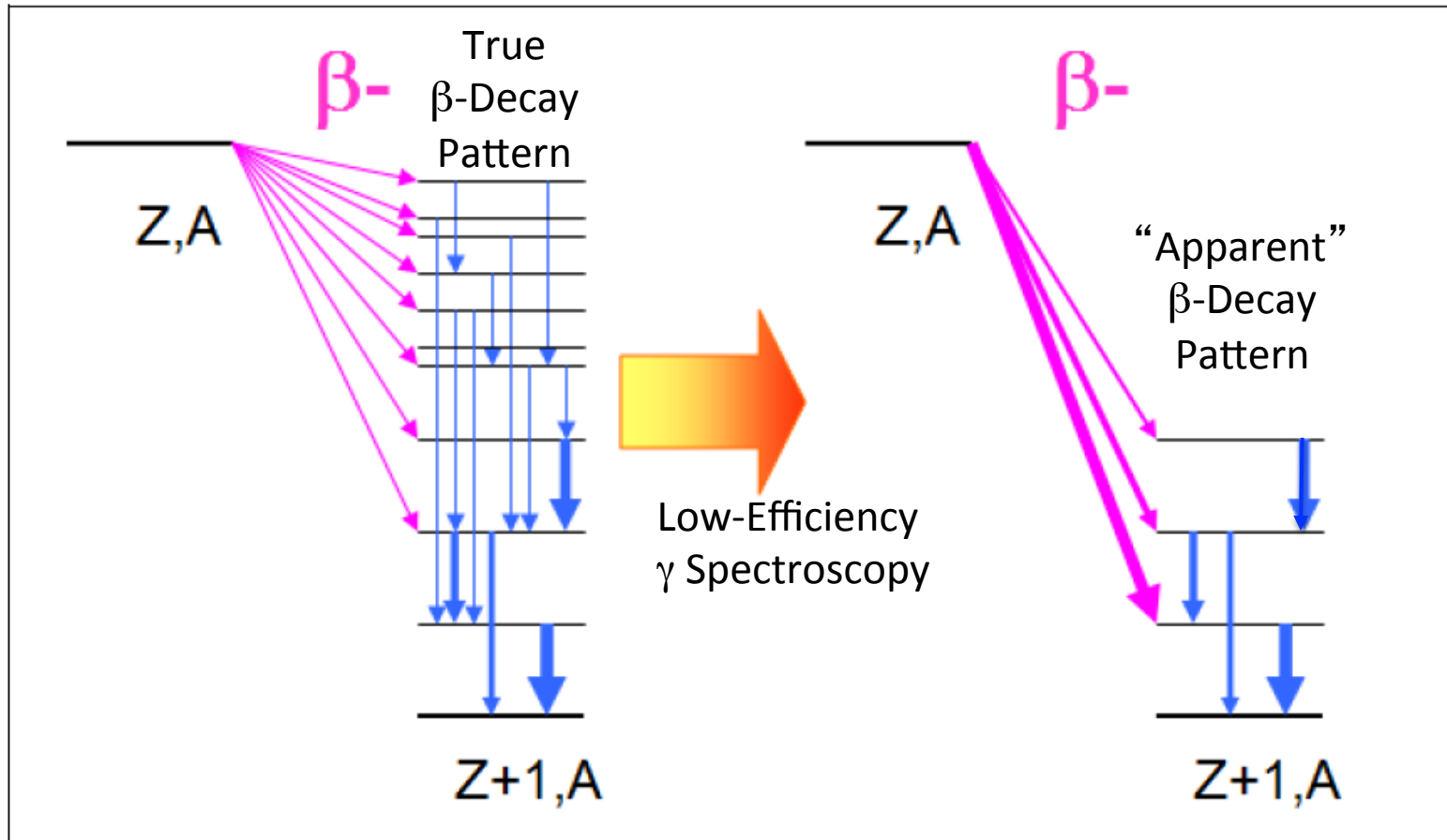
VANDLE



3Hen



The Pandemonium Effect

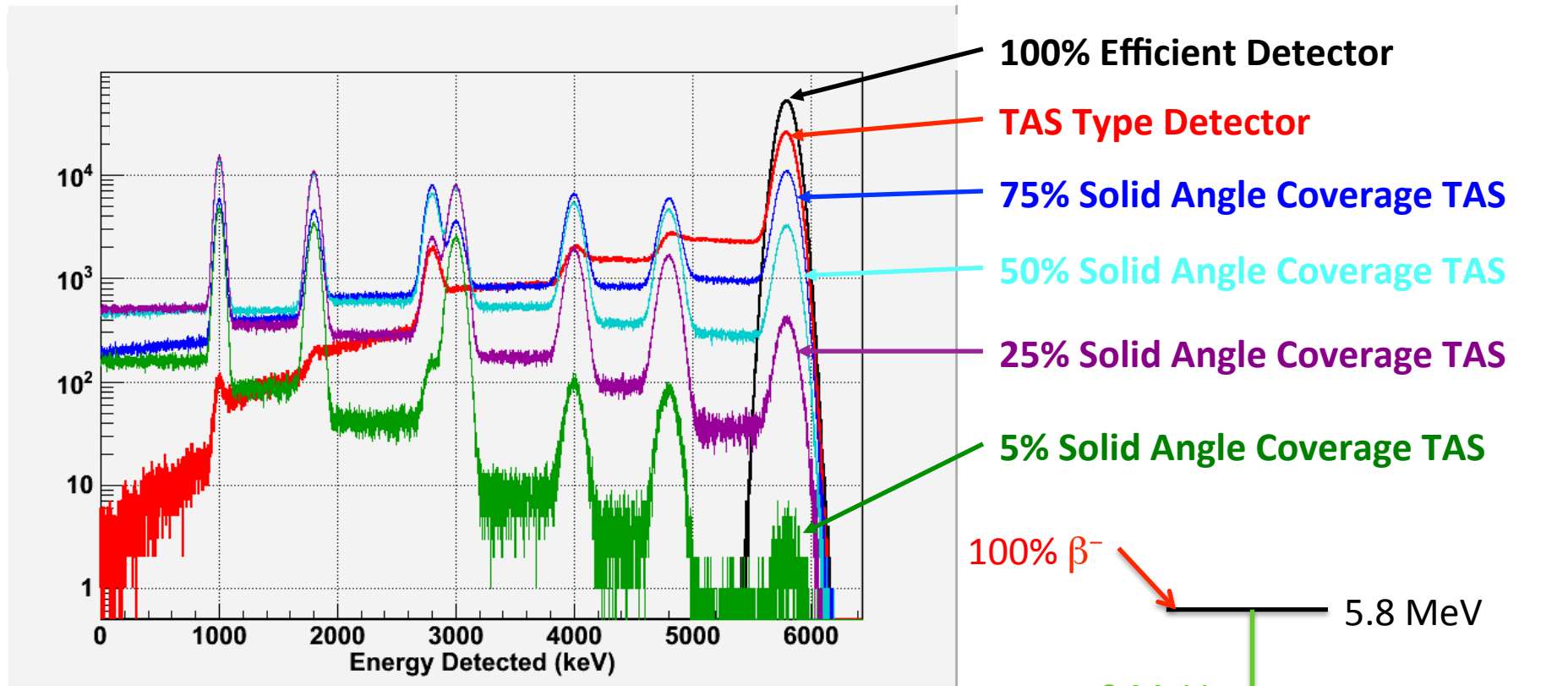


A.A. Sonzogni and M. Herman, NNDC 2011

Adopting “Apparent” decay pattern results in a wrong interpretation of β decay properties and respective nuclear structure. The energies and intensities of emitted γ -rays are underestimated while β -electron and neutrino energies are over estimated.

Total Absorption Spectrometry (TAS) is the Solution!

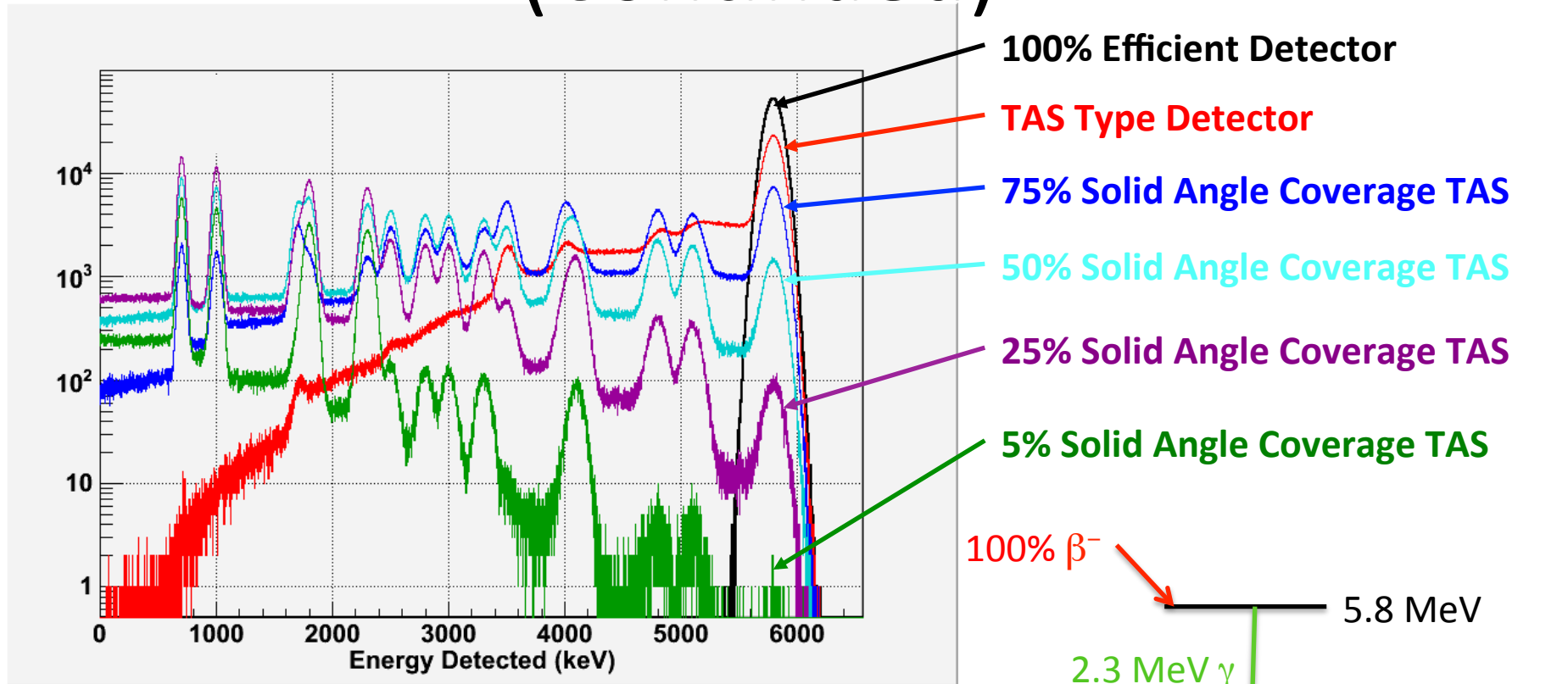
Illustration of the Pandemonium Effect



Simulated 3 γ Decay from a Hypothetical 5.8 MeV Level

($E_\gamma=1$ MeV, 1.8 MeV, and 3 MeV)

Illustration of the Pandemonium Effect (Continued)



Simulated 4 γ Decay from a Hypothetical 5.8 MeV Level

($E_\gamma = 700$ keV, 1 MeV, 1.8 MeV, and 2.3 MeV)

Current and Previous TAS Detectors

Modular Total Absorption Spectrometer (MTAS)

ORNL (since ~2011)

Idaho TAS : (1990' s → ANL)

MTAS has 17 times larger volume

LBNL TAS : GSI (1995 – 2003) → LBNL

MTAS is 7 times larger

Valencia-ISOLDE “Lucrecia” TAS (since ~2003)

MTAS is 8 times larger

MSU-Notre Dame “SuN” TAS (since ~2011)

MTAS is 5 times larger

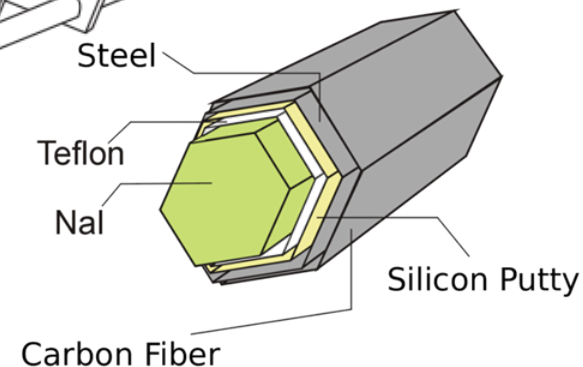
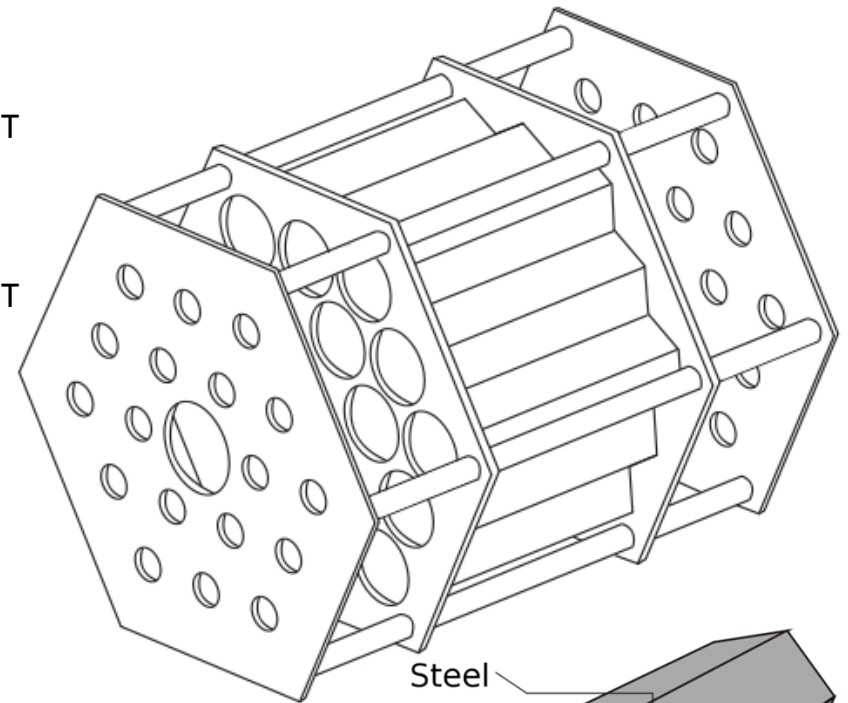
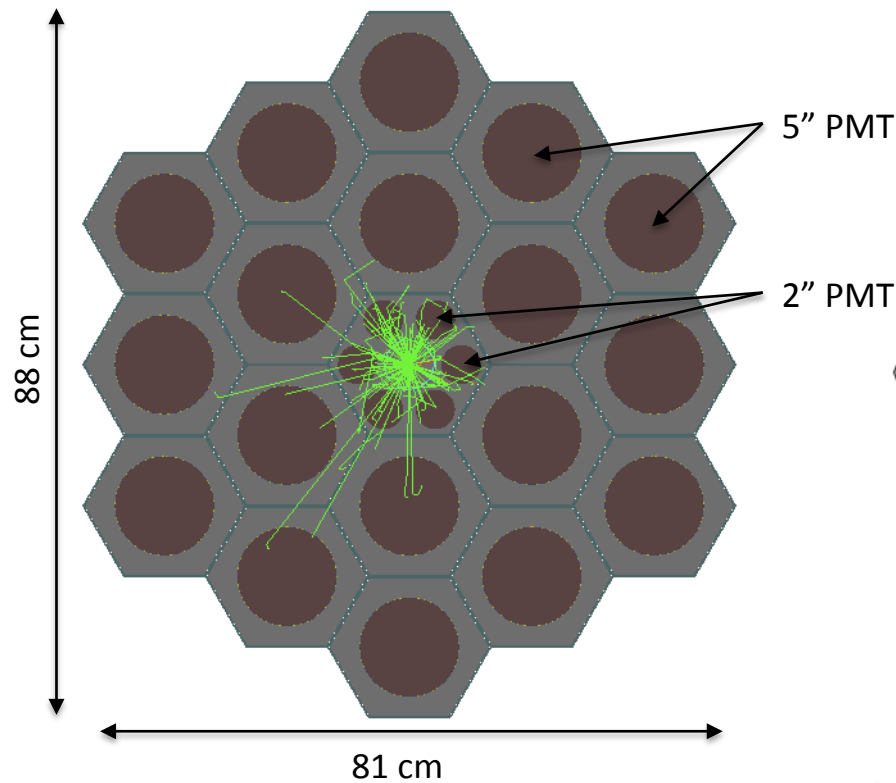
Modular Total Absorption Spectrometer

19 Hexagonal NaI(Tl) Modules (53.3 cm x 17.6 cm Face to Face) with Carbon Fiber Housing

Each Regular Module has 2-5" PMT, while the Center Module has 12-2" PMT

Center Module has 6.35 cm Hole to Accommodate Beam Line and Auxiliary β -Detectors

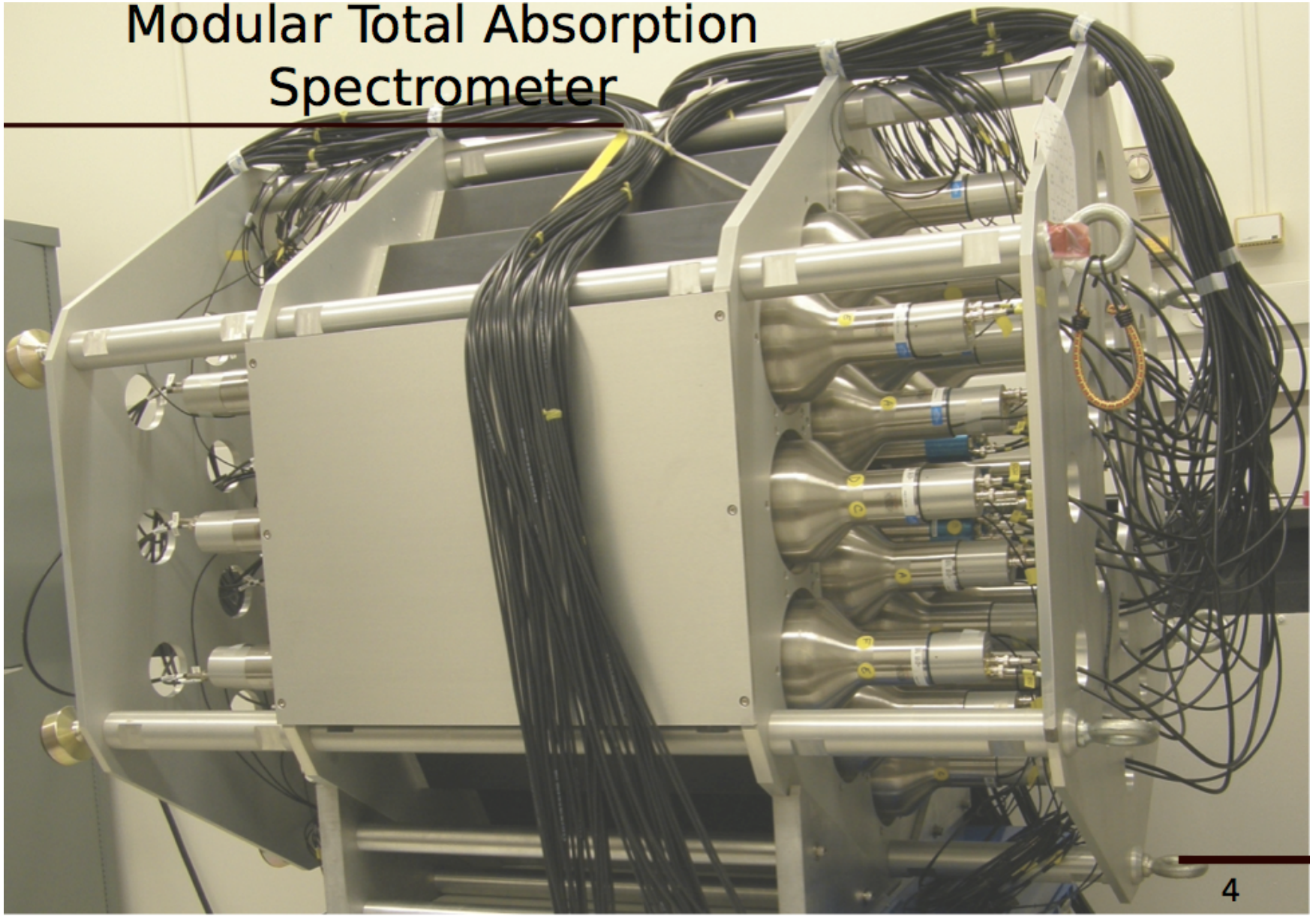
Approximately **One Ton** of NaI(Tl)!



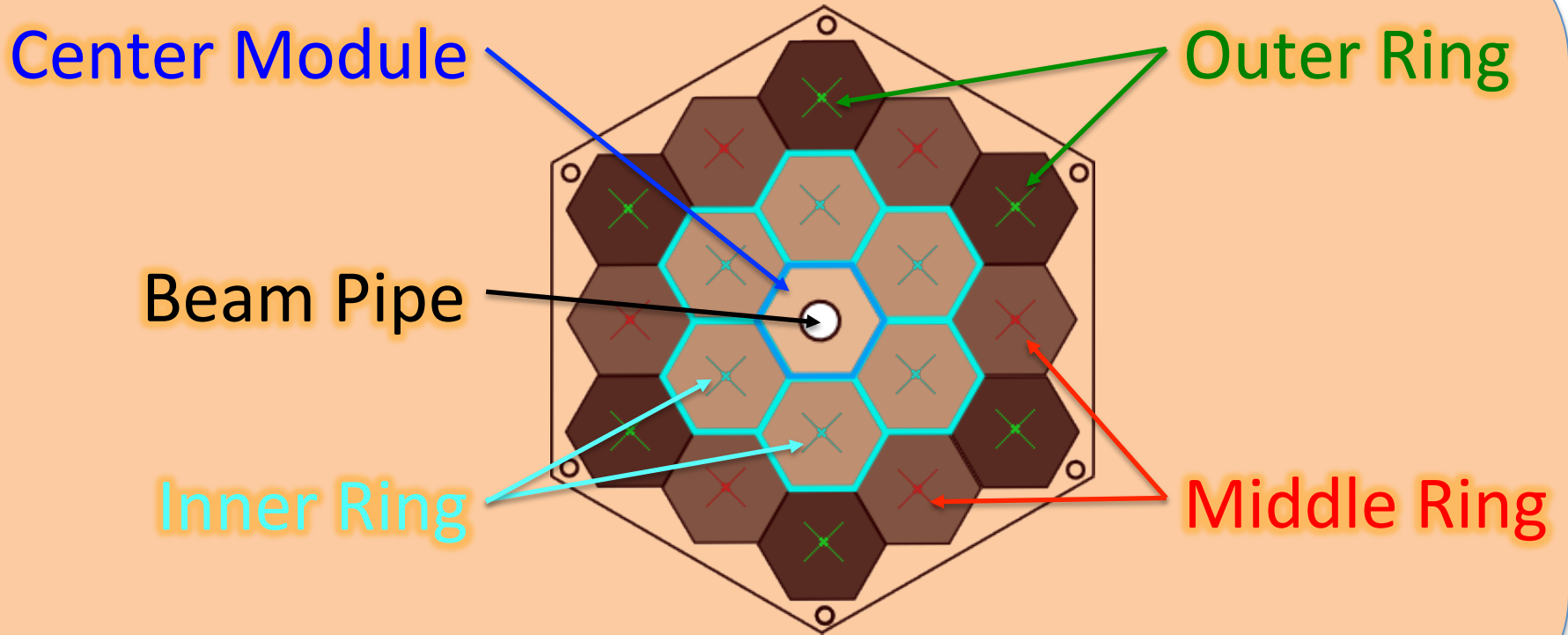
Modular Total Absorption Spectrometer with
100 ^{137}Cs Simulated Decays

MTAS

Modular Total Absorption
Spectrometer

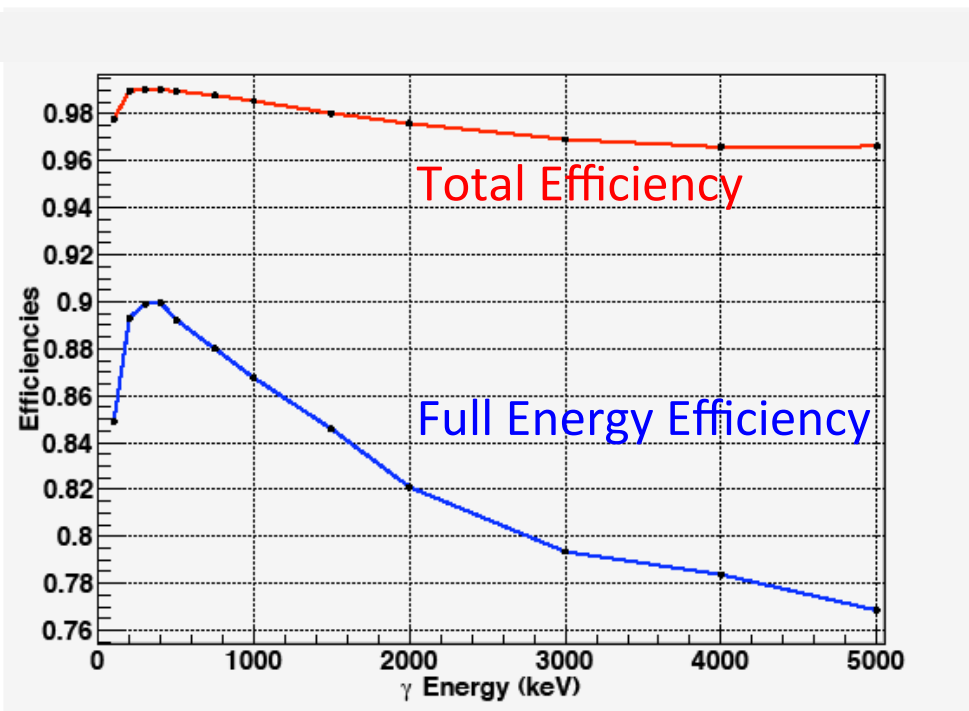


MTAS Ring Identification

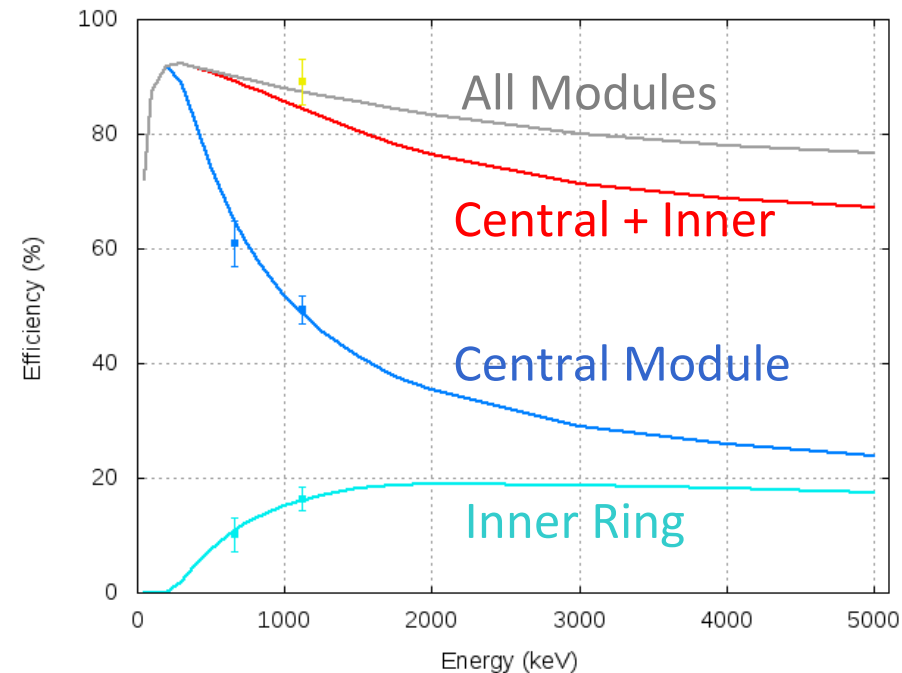


Efficiency of MTAS

Single γ Total Efficiency and Single γ Full Energy (Peak) Efficiency are Critical Parameters for Total Absorption Spectrometry (TAS)

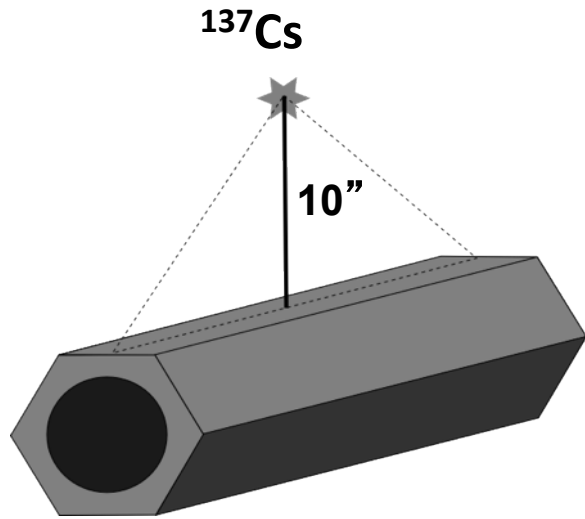


Simulated Single γ -Ray Efficiency versus Energy
Total Efficiency: Any Energy Deposited
Full Energy (Peak) Efficiency: All Energy Deposited

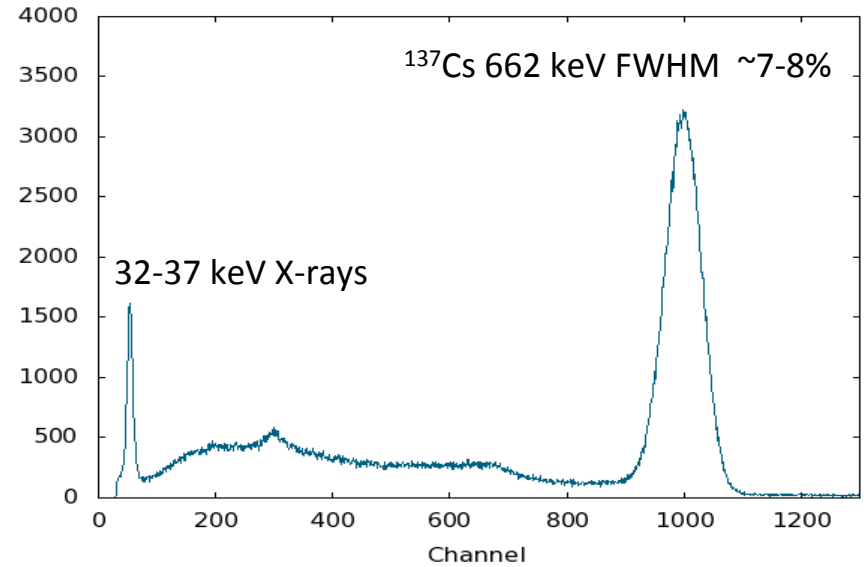


Single γ -Ray Full Energy Efficiency by Ring
Also Shown are ^{137}Cs and ^{65}Zn Data

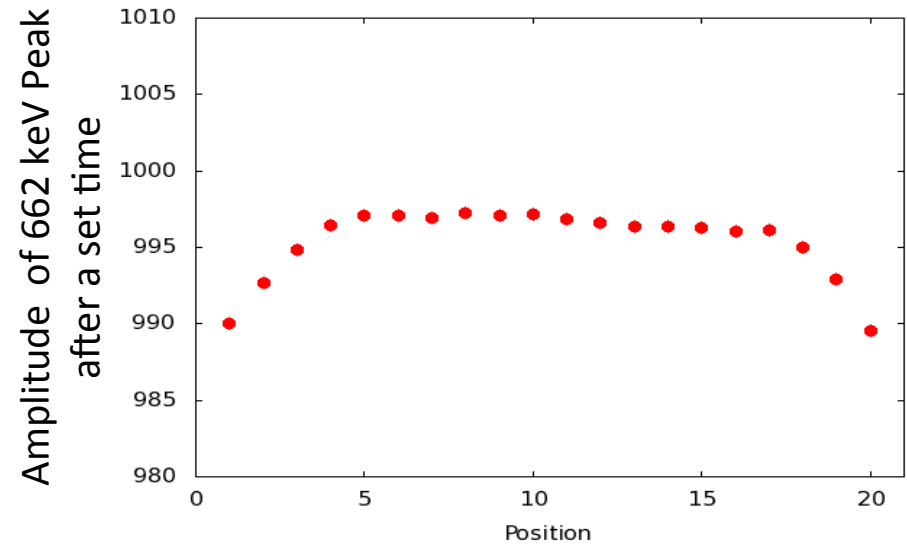
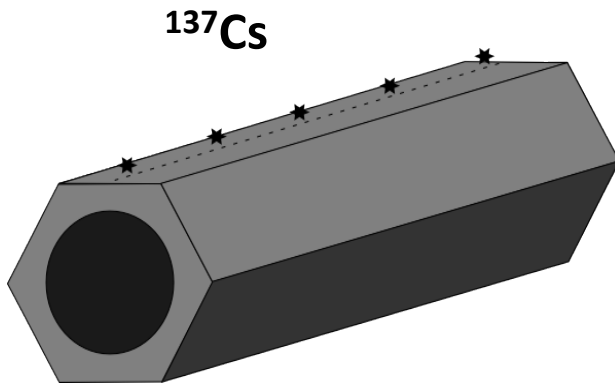
Test Measurements with ^{137}Cs Source



St Gobain specifications: FWHM < 8.5%

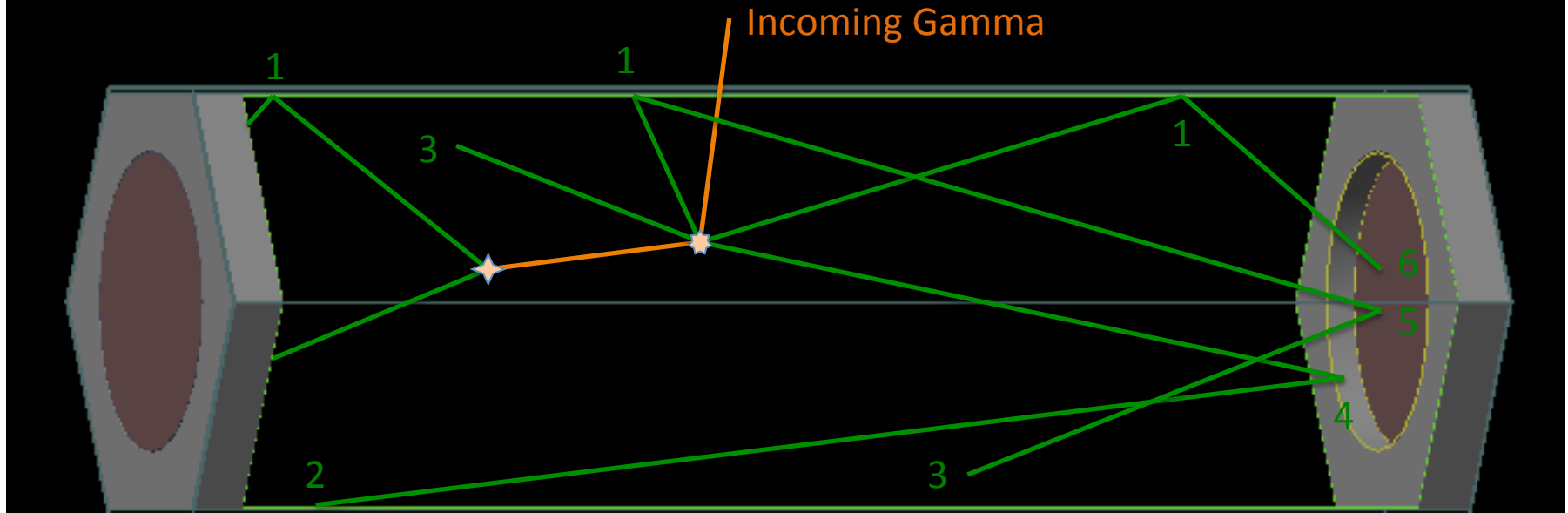


Uniformity of modules was measured with ^{137}Cs source placed along each side (19 measurements per each side, 1" steps)



Simulation of Light Production in NaI(Tl)

Contributing Factors to Energy Resolution



Green Are Optical Photons Generated by Electrons (Select Few for Illustration Purposes)

★ Photoelectric Absorption

★ Compton Scattering

1 – Reflection at Teflon NaI Boundary

4 – Reflection at NaI Window Glass Boundary

2 – Absorption at Teflon NaI Boundary

5 – Reflection at PMT Cathode Face

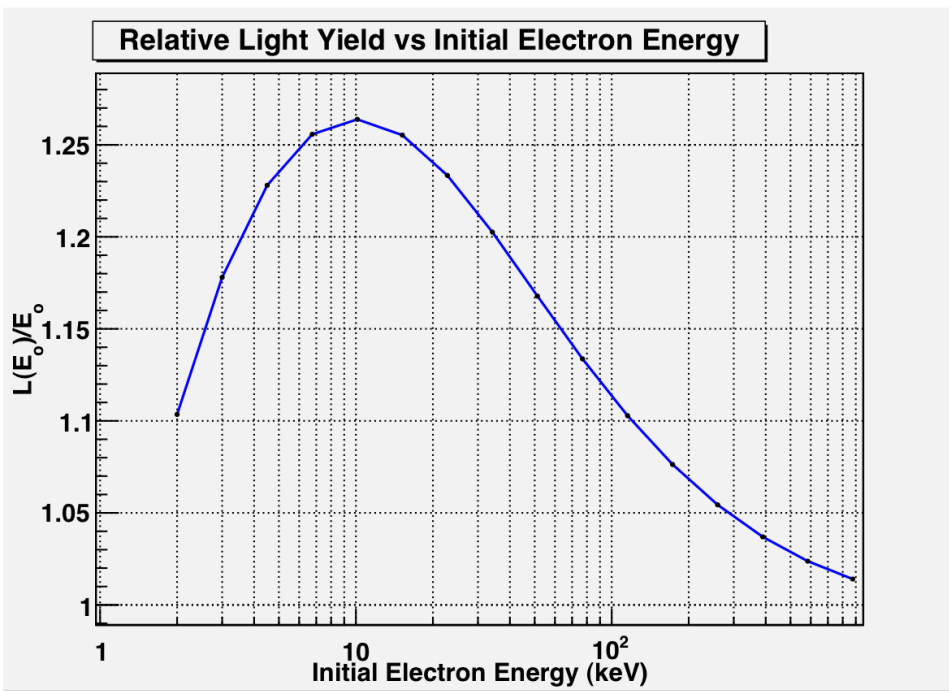
3 – Absorption by NaI Crystal

6 – Absorption with PE Creation on PMT Face

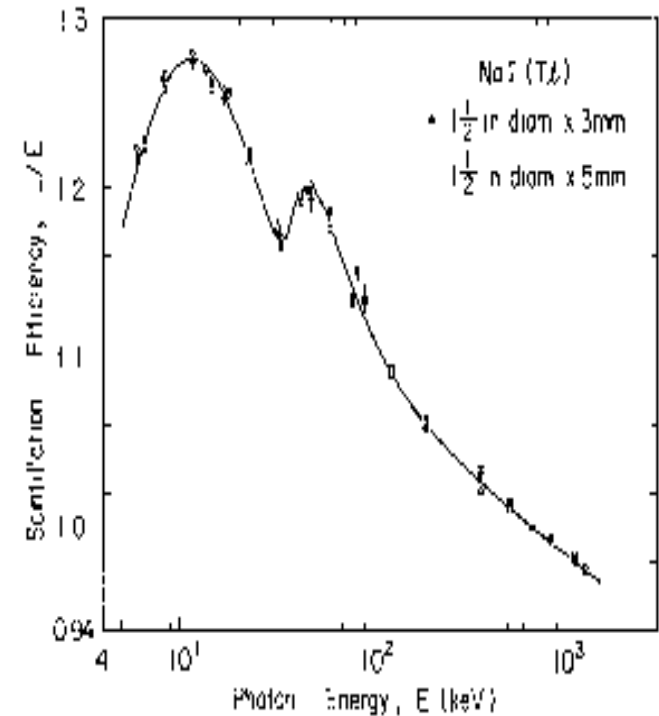
+ Nonlinear Light Production!

Nonlinear Light Generation in NaI(Tl)

Scintillators generate light approximately proportional to the energy deposited. But at low energy this is not necessarily the case. Organic scintillators often see a decrease in light output per energy deposited. NaI(Tl) actually generates an excess of light for energies less than ~ 1 MeV.



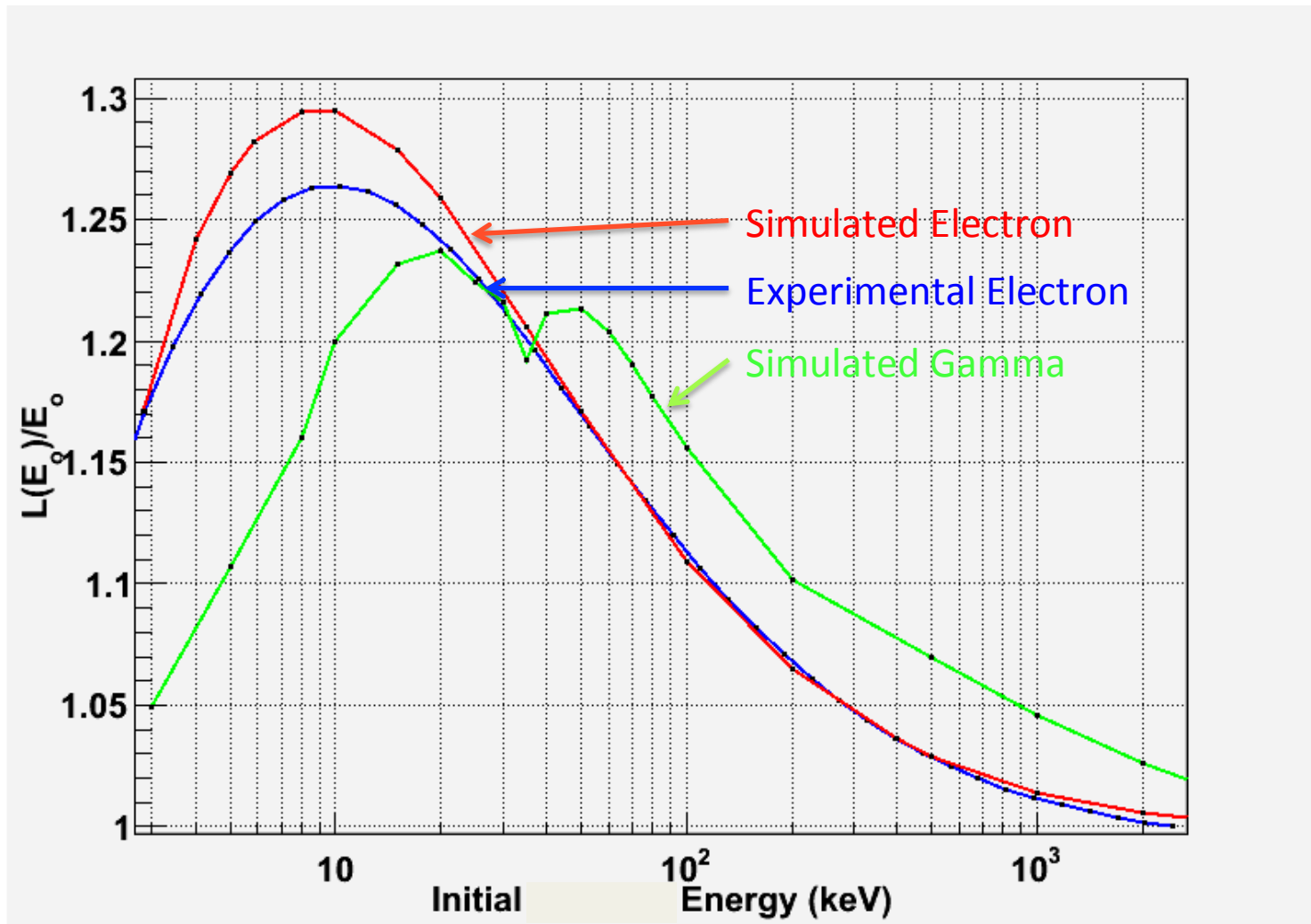
Parameterized experimental light output of electrons of a specified initial energy. The curve is normalized to unity for 3 MeV electrons.



Experimental light output of γ rays versus initial energy. The curve is normalized to unity at 662 keV. T. Tojo, NIM A238 (1985)

Simulation of Light Production in NaI(Tl)

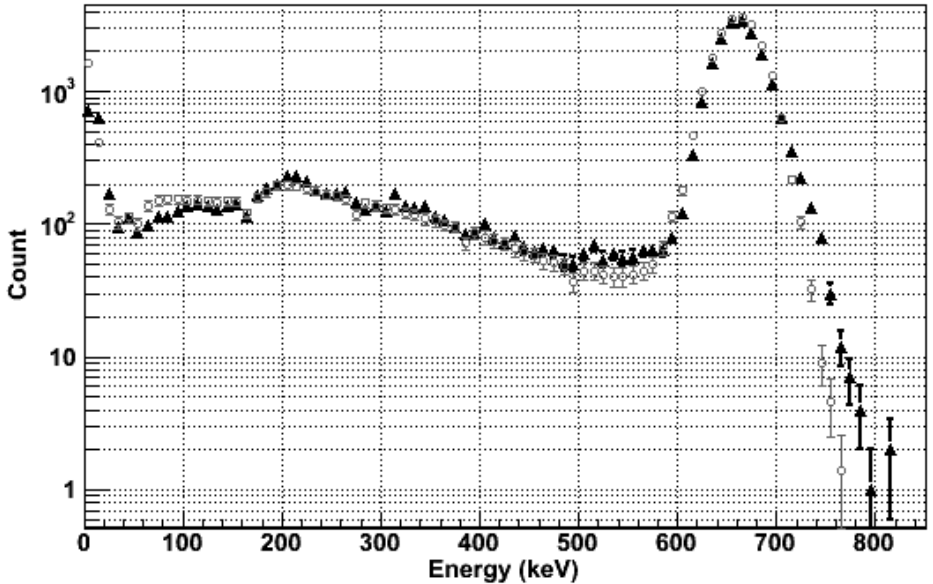
Nonlinear Light Generation



Results from dE/dx based light production in GEANT4. Good results for particles above ~ 20 keV.

Simulation Compared to Measurement

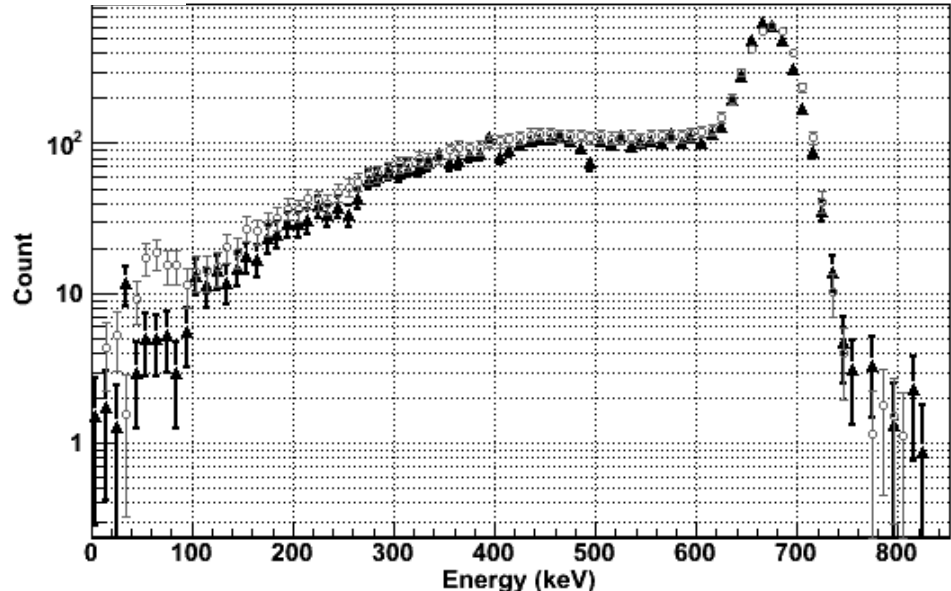
Center Module



Low Activity ^{137}Cs

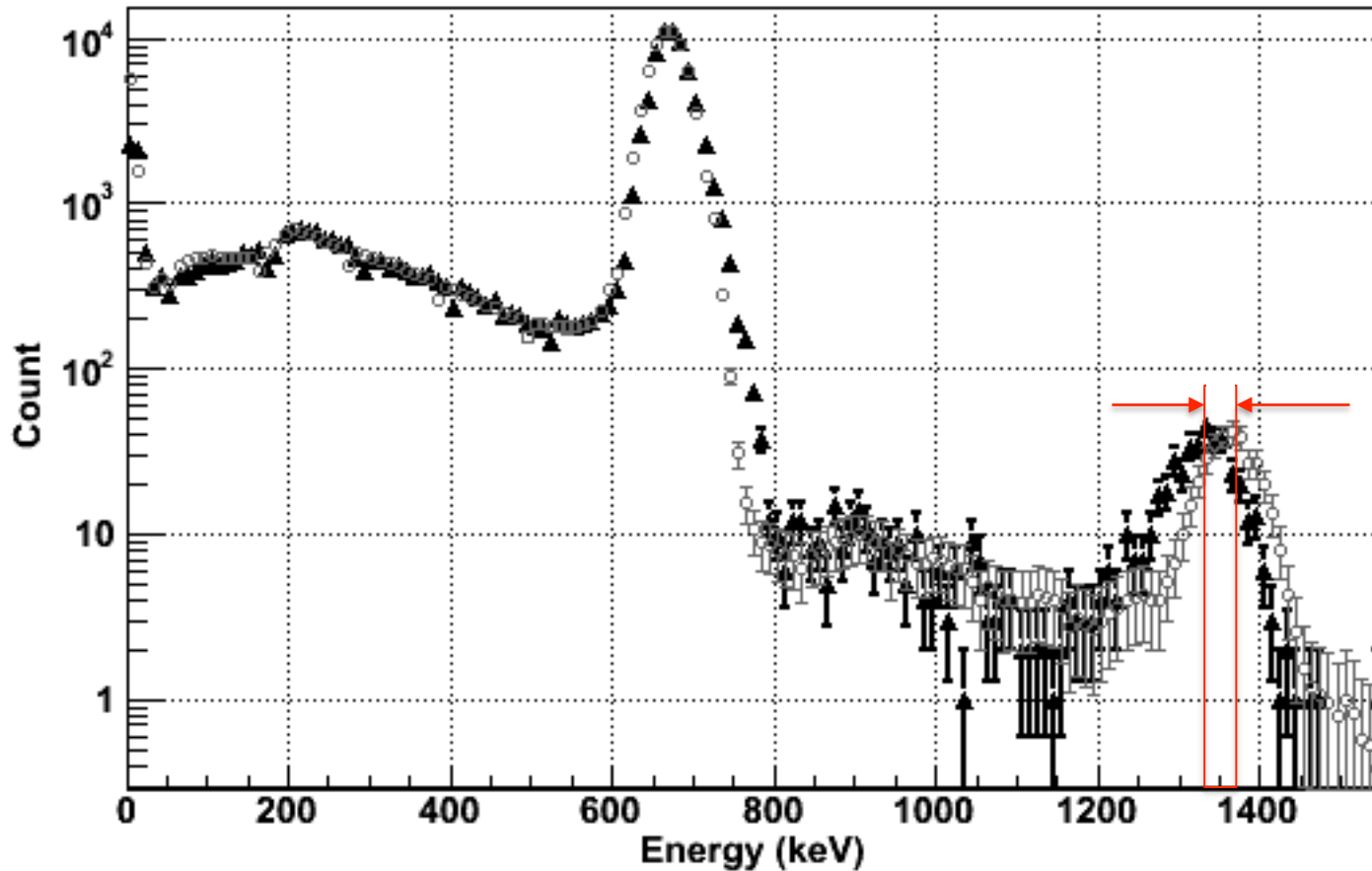
Triangles – Simulation
Open Circles - Data

Inner Ring



Simulation Compared to Measurement

High Activity ^{137}Cs Center Module

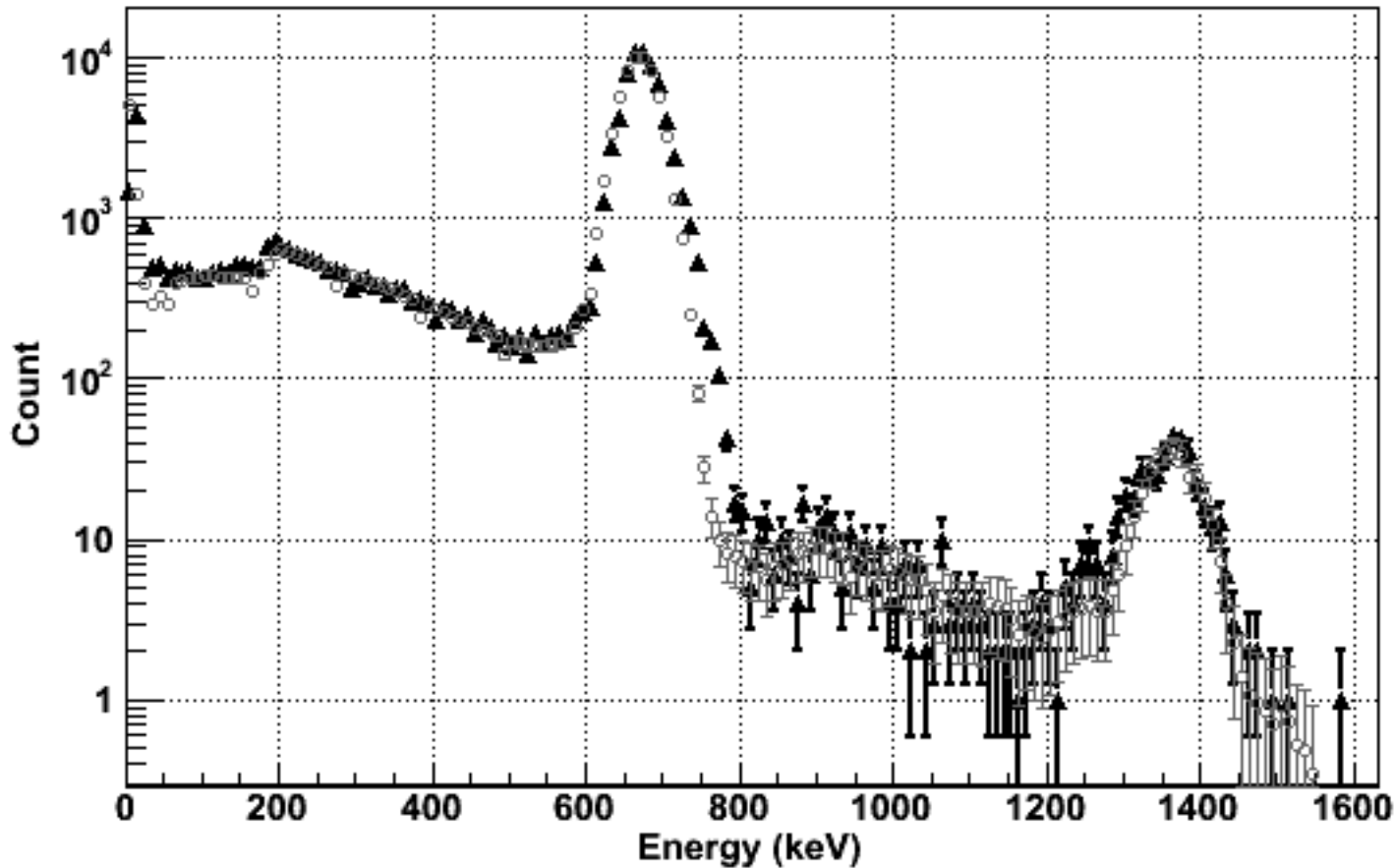


Triangles – Simulation
Open Circles - Data

Per PMT Channel for Each Additional γ in Multi- γ Decays
 ~ 3 keV Shift per PMT per extra γ in Center Module (2.5" PMT)
 ~ 7 keV Shift per PMT per extra γ for Other Modules (5" PMT)

Simulation Compared to Measurement

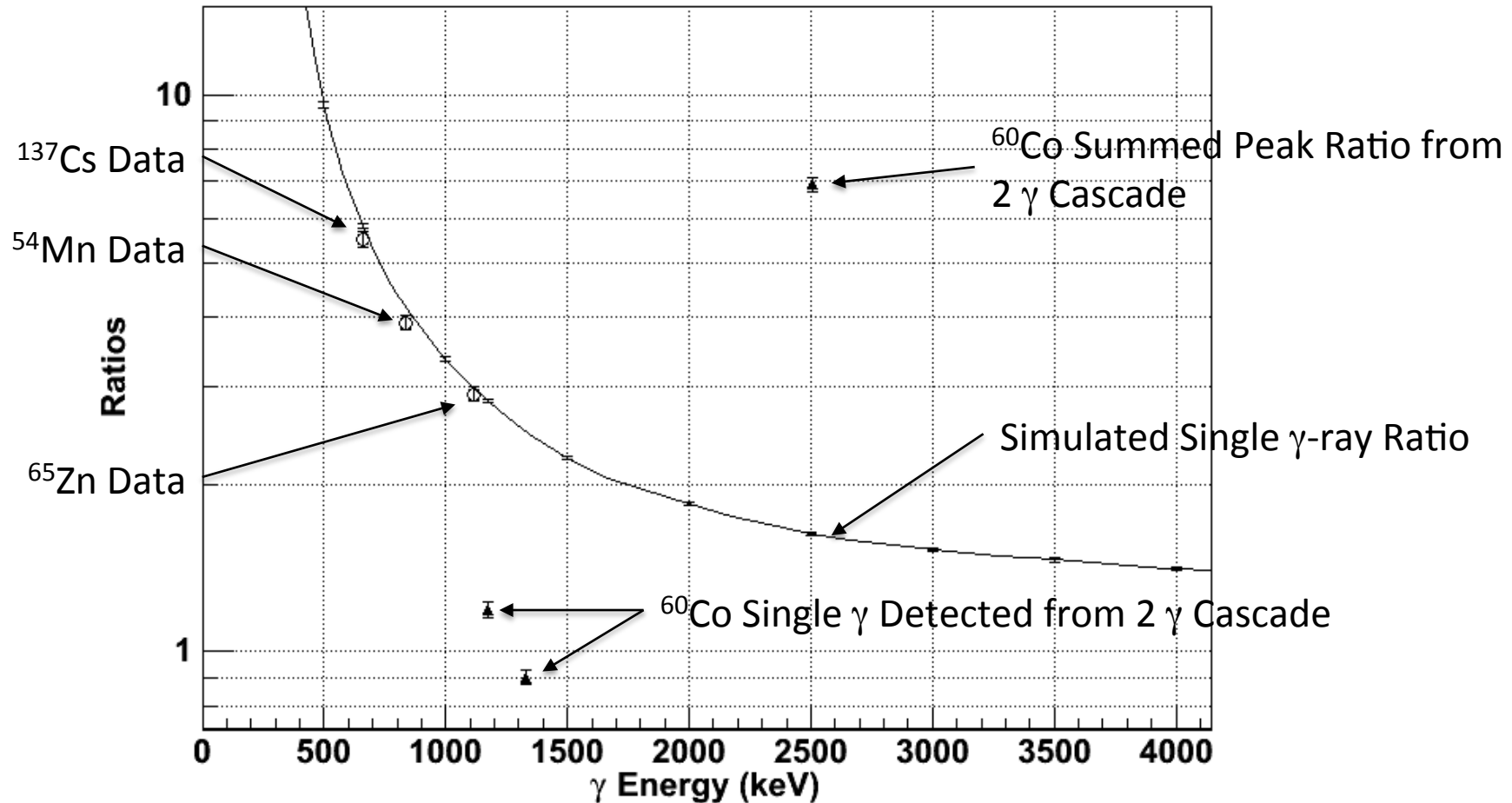
High Activity ^{137}Cs Center Module



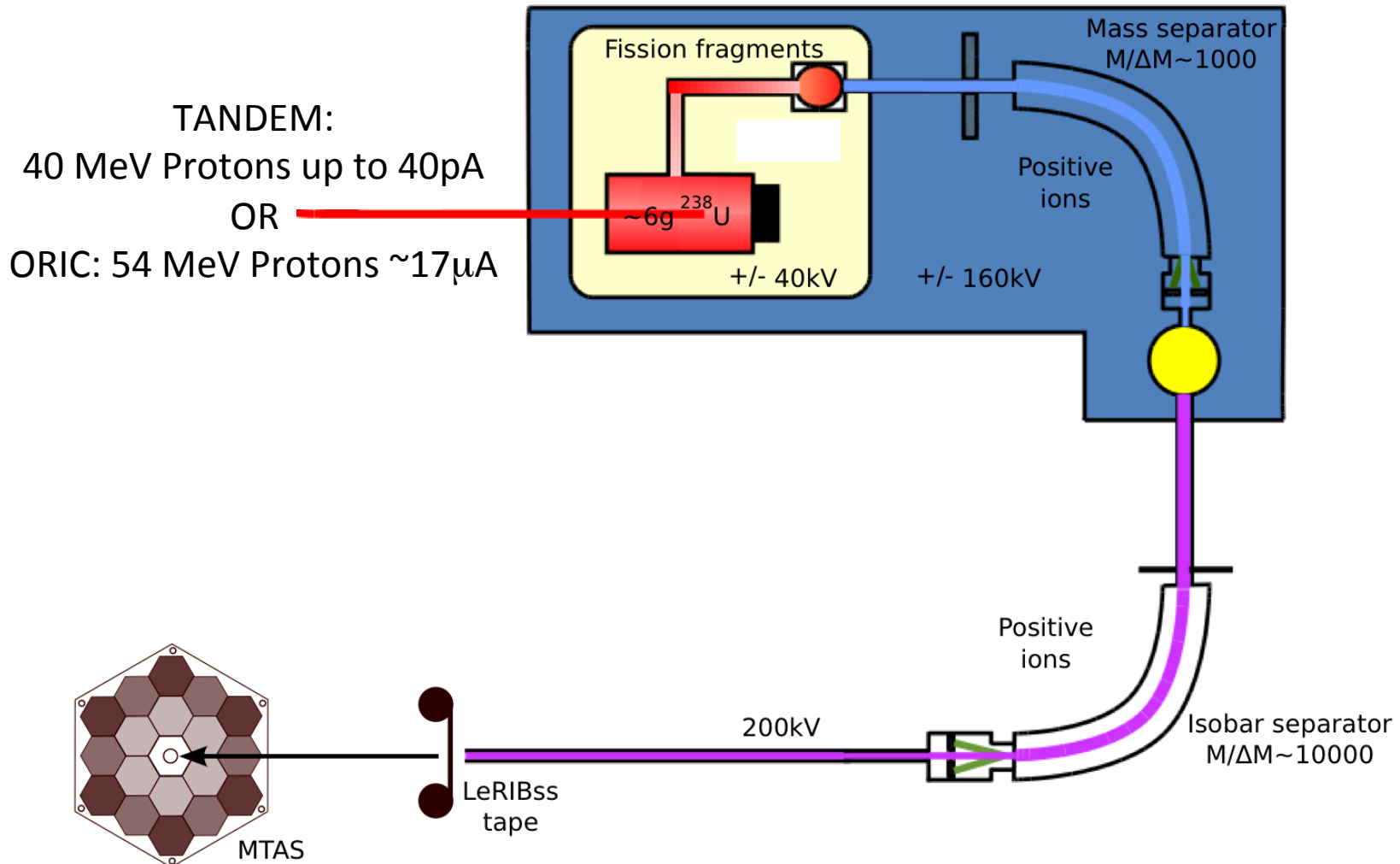
Triangles – Simulation
Open Circles - Data

Modularity Uses of MTAS

Ratio of the counts in the central detector versus the inner ring of modules gives a measure of the γ multiplicity of the event

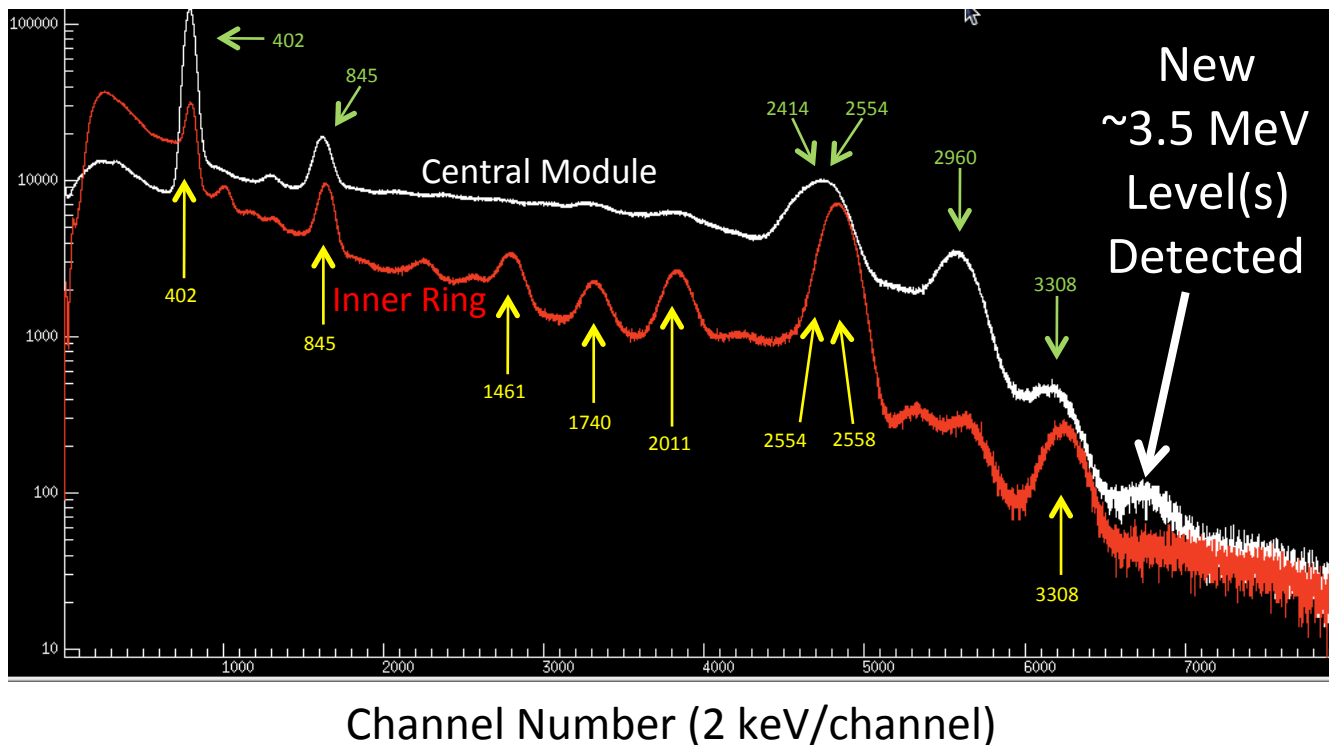


MTAS Experimental Setup



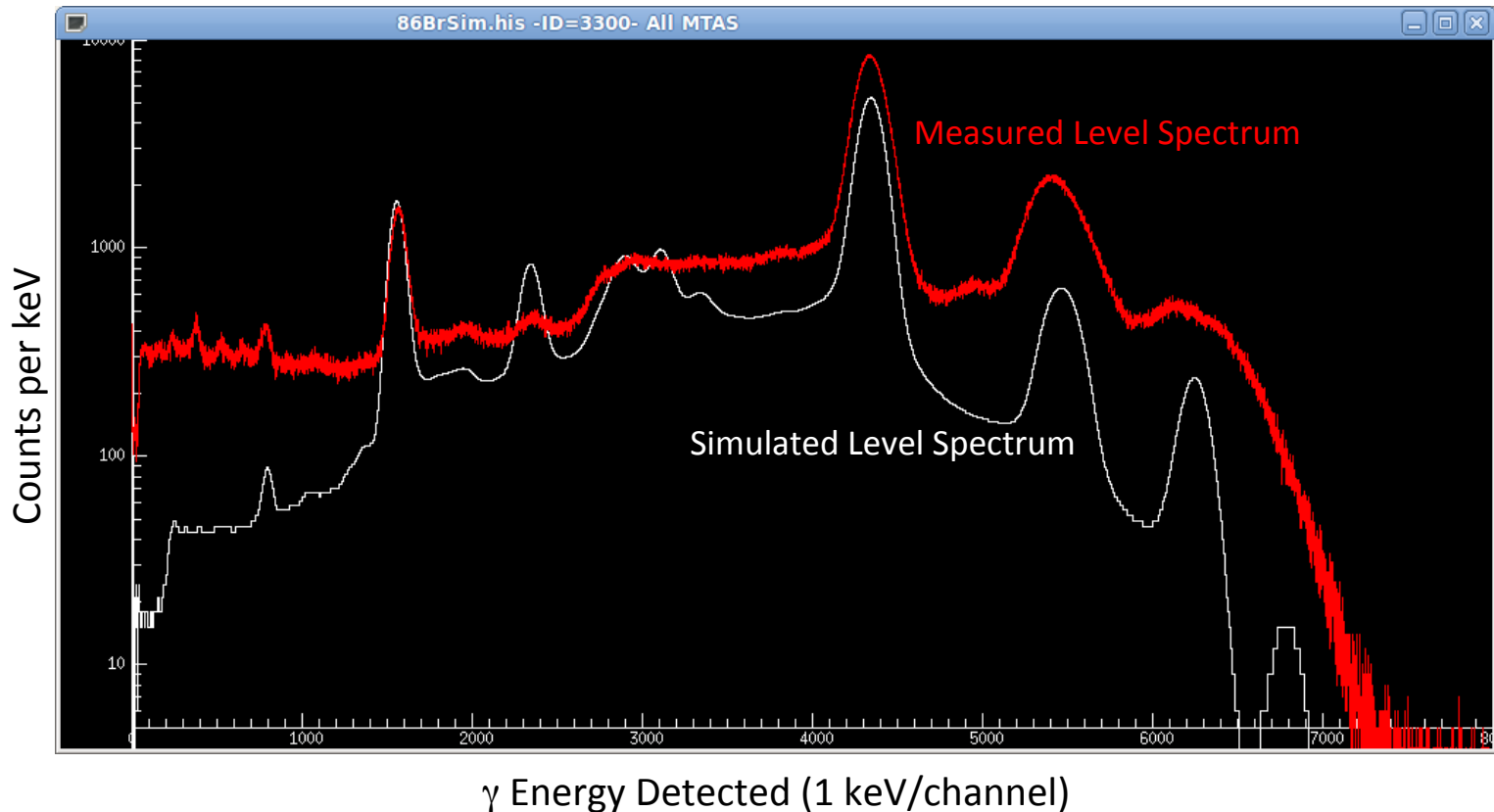
First MTAS measurement of ^{87}Kr radioactivity ($T_{1/2}=76$ min) at the HRIBF

A=87 mass chain ending with ^{87}Kr decay is produced
in thermal neutron fission at the rate of 2.5% per ^{235}U and 1% per ^{239}Pu



MTAS at the HRIBF's OLTF, January 2012

Example of Collected Data: Priority "1" Decay of $^{86}\text{Br} \rightarrow ^{86}\text{Kr} + \beta^-$



The measured MTAS gamma spectrum (red line) is compared to the simulation of MTAS response (white line) to the decay of ^{86}Br listed in the adopted data files. The normalization is made to match the feeding of the 1.6 MeV excited state in ^{86}Kr . An excess of high energy gamma radiation release is clearly detected
(A. Kuźniak et al., January 2012, preliminary)

International Evaluation Co-operation

VOLUME 25

ASSESSMENT OF FISSION PRODUCT
DECAY DATA FOR DECAY HEAT CALCULATIONS

A report by the Working Party
on International Evaluation Co-operation
of the NEA Nuclear Science Committee

CO-ORDINATOR

T. Yoshida
Musashi Institute of Technology
JAPAN

MONITOR

A.L. Nichols
International Atomic Energy Agency
AUSTRIA

Red Arrows Indicate Recent
MTAS-OLTF Measurements

Y88 106.65 d	Y89	Y90 64.00 h	Y91 58.51 d	Y92 3.54 h	Y93 10.18 h	Y94 18.7 m	Y95 10.3 m
Sr87	Sr88	Sr89 50.53 d	Sr90 28.79 y	Sr91 9.63 h	Sr92 2.66 h	Sr93 7.42 m	Sr94 75.3 s
Rb86 18.64 d	Rb87	Rb88 17.78 m	Rb89 15.15 m	Rb90 158 s	Rb91 58.4 s	Rb92 4.49 s	Rb93 5.84 s
Kr85 10.77 y	Kr86	Kr87 76.3 m	Kr88 2.84 h	Kr89 3.15 m	Kr90 32.32 s	Kr91 8.57 s	Kr92 1.84 s
Br84 31.80 m	Br85 2.90 m	Br86 55.1 s	Br87 55.65 s	Br88 16.36 s	Br89 4.40 s	Br90 1.91 s	Br91 541 ms
Se83 22.3 m	Se84 3.1 m	Se85 31.7 s	Se86 15.3 s	Se87 5.50 s	Se88 1.53 s	Se89 410 ms	Se90 300 ms
As82 19.1 s	As83 13.4 s	As84 4.02 s	As85 2.02 s	As86 945 ms	As87 610 ms	As88 300 ms	As89 200 ms

La138	La139	La140 1.67 d	La141 3.92 h	La142 91.1 m	La143 14.2 m
Ba137	Ba138	Ba139 83.1 m	Ba140 12.75 d	Ba141 18.27 m	Ba142 10.6 m
Cs136 13.16 d	Cs137 30.16 y	Cs138 33.41 m	Cs139 9.27 m	Cs140 63.7 s	Cs141 24.84 s
Xe135 9.14 h	Xe136	Xe137 3.81 m	Xe138 14.08 m	Xe139 39.68 s	Xe140 13.60 s
I134 52.5 m	I135 6.57 h	I136 83.4 s	I137 24.13 s	I138 6.23 s	I139 2.28 s
Te133 12.5 m	Te134 41.8 m	Te135 19.0 s	Te136 17.63 s	Te137 2.49 s	Te138 1.4 s

Radionuclide	Priority	Q_{β} -value (keV)	Half-life	Comments
35-Br-86	1	7626(11)	55.1 s	
35-Br-87	1	6852(18)	55.65 s	Extremely complex decay scheme with substantial gamma component; large uncertainties in the mean gamma energy arises from significant disagreements between the various discrete gamma-ray measurements. Also (β^- , n) branch.
35-Br-88	1	8960(40)	16.36 s	(β^- , n) branch.
36-Kr-89	1	4990(50)	3.15 min	Incomplete decay scheme.
36-Kr-90	1	4392(17)	32.32 s	Incomplete decay scheme.
37-Rb-90m	2	6690(15)	258 s	Repeat of INL TAGS measurement; data check.
37-Rb-92	2	8096(6)	4.49 s	Small (β^- , n) branch.
38-Sr-89	2	1493(3)	50.53 d	
38-Sr-97	2	7470(16)	0.429 s	Extremely short half-life (0.429 s), and possible (β^- , n) branch.
39-Y-96	2	7096(23)	5.34 s	
40-Zr-99	3	4558(15)	2.1 s	
40-Zr-100	2	3335(25)	7.1 s	
41-Nb-98	1	4583(5)	2.86 s	
41-Nb-99	1	3639(13)	15.0 s	
41-Nb-100	1	6245(25)	1.5 s	
41-Nb-101	1	4569(18)	7.1 s	
41-Nb-102	2	7210(40)	1.3 s	
42-Mo-103	1	3750(60)	67.5 s	
42-Mo-105	1	4950(50)	35.6 s	
43-Tc-102	1	4532(9)	5.28 s	
43-Tc-103	1	2662(10)	54.2 s	
43-Tc-104	1	5600(50)	18.3 min	
43-Tc-105	1	3640(60)	7.6 min	
43-Tc-106	1	6547(11)	35.6 s	
43-Tc-107	2	4820(90)	21.2 s	
51-Sb-132	1	5509(14)	2.79 min	
52-Te-135	2	5960(90)	19.0 s	

Radionuclide	Priority	Q_{β} -value (keV)	Half-life	Comments
53-I-136	1	6930(50)	83.4 s	Incomplete decay scheme.
53-I-136m	1	7580(120)	46.9 s	
53-I-137	1	5877(27)	24.13 s	(β^- , n) branch.
54-Xe-137	1	4166(7)	3.82 min	Incomplete decay scheme.
54-Xe-139	1	5057(21)	39.68 s	
54-Xe-140	1	4060(60)	13.6 s	
55-Cs-142	3	7308(11)	1.69 s	(β^- , n) branch.
56-Ba-145	2	5570(110)	4.31 s	Repeat of INL TAGS measurement; data check.
57-La-143	2	3425(15)	14.2 min	Repeat of INL TAGS measurement; data check.
57-La-145	2	4110(80)	24.8 s	Repeat of INL TAGS measurement; data check.

MTAS Collaborators

K.P. Rykaczewski¹, C.J. Gross¹, R.K. Grzywacz^{1,3}, J. Johnson¹, A. Kuźniak^{2,3}, M. Karny^{1,2,4},
D.Miller³, B.C. Rasco⁵, D.Stracener¹, M. Wolińska-Cichocka^{1,4}, E. Zganjar⁵

¹ORNL, Oak Ridge, TN 37830, USA,

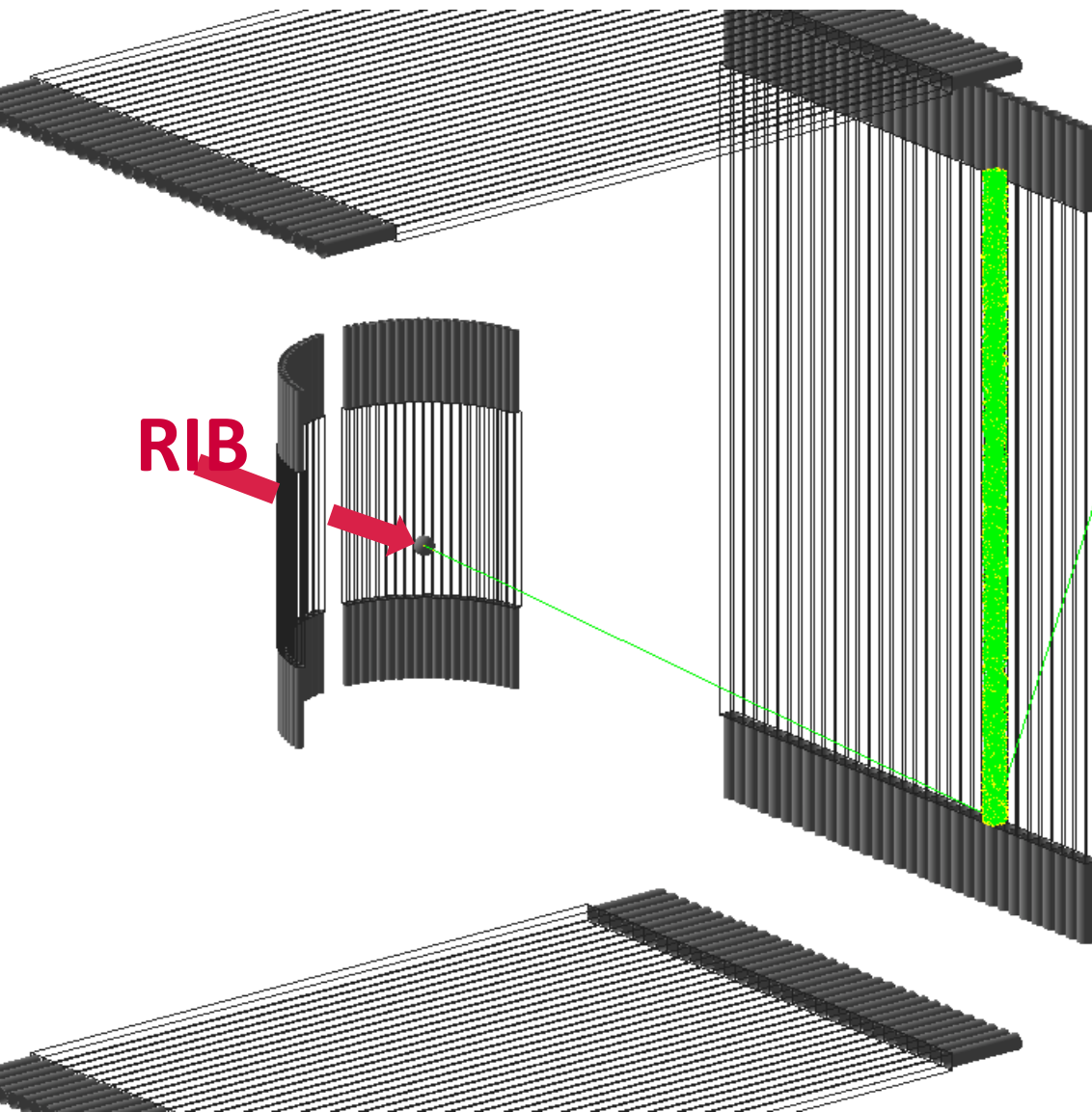
²University of Warsaw, Warsaw, PL 00-681, Poland,

³University of Tennessee, Knoxville, TN 37996, USA,

⁴ORAU, Oak Ridge, TN 37830, USA,

⁵Louisiana State University, Baton Rouge, LA 70803, USA

Versatile Array of Neutron Detectors at Low Energy (VANDLE)



Neutron Time of Flight Detector

~250 Configurable Scintillator
(BC408) Bars

Two sizes of Scintillator Bars:

200 cm length (5^2 cm² area)

60 cm length (2.5^2 cm² area)

Bars can be arranged in different configurations that are optimized for particular types of measurements including transfer reactions like (d,n) and neutron emission following β decay

VANDLE

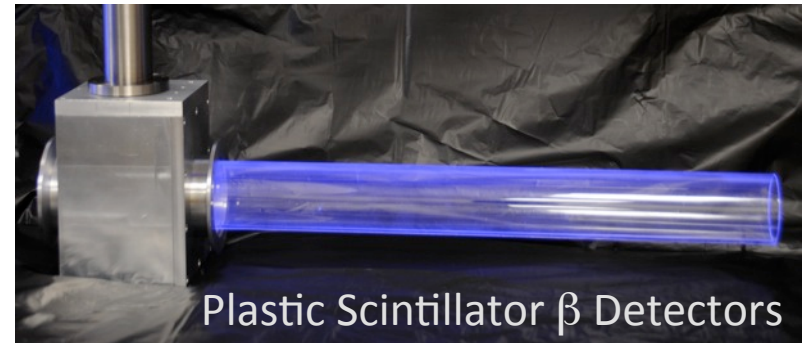
First VANDLE Experimental Setup

Time of Flight Neutron and γ Detector

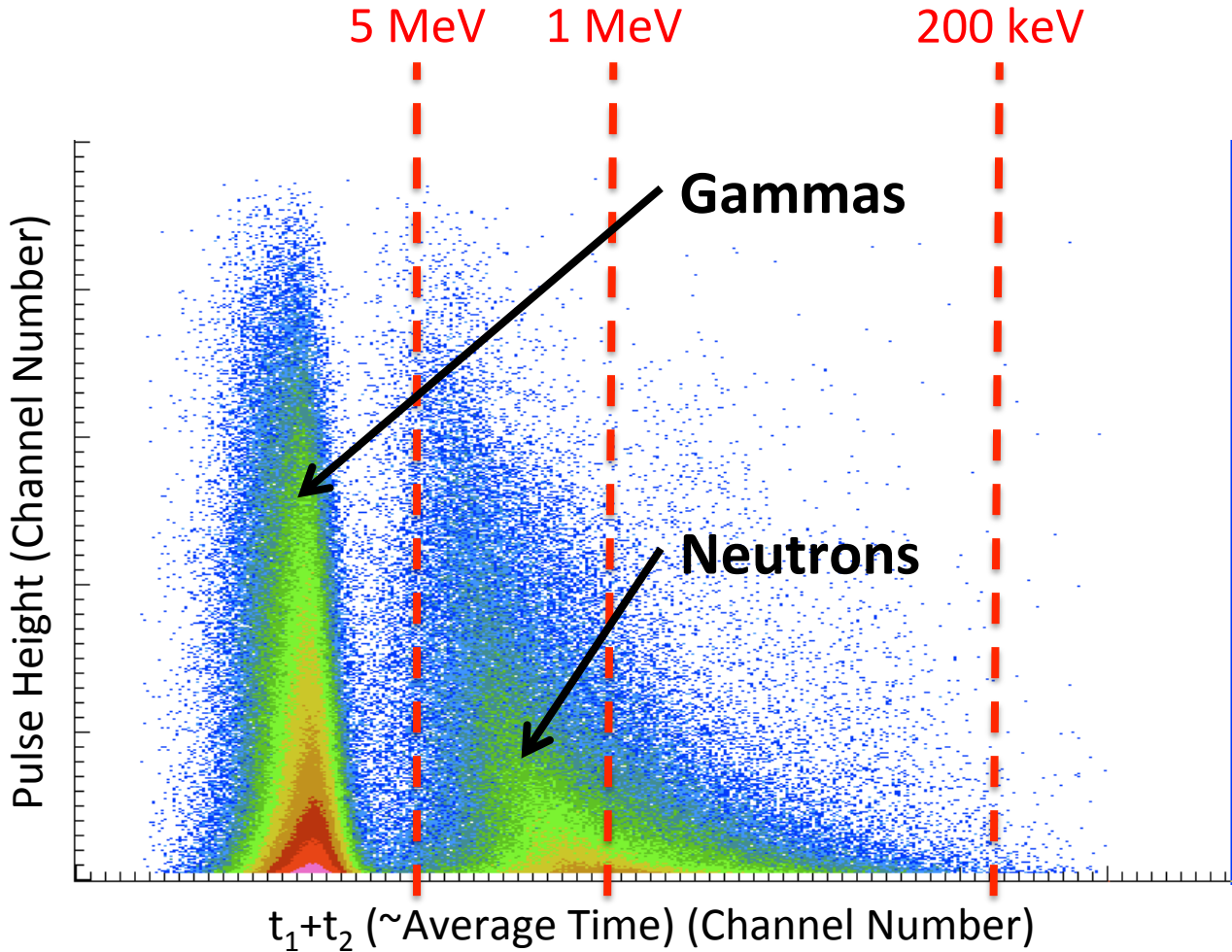
40 – 60 x 2.5 x 2.5 cm³ Scintillator Bars

2 Clover Germanium Detector

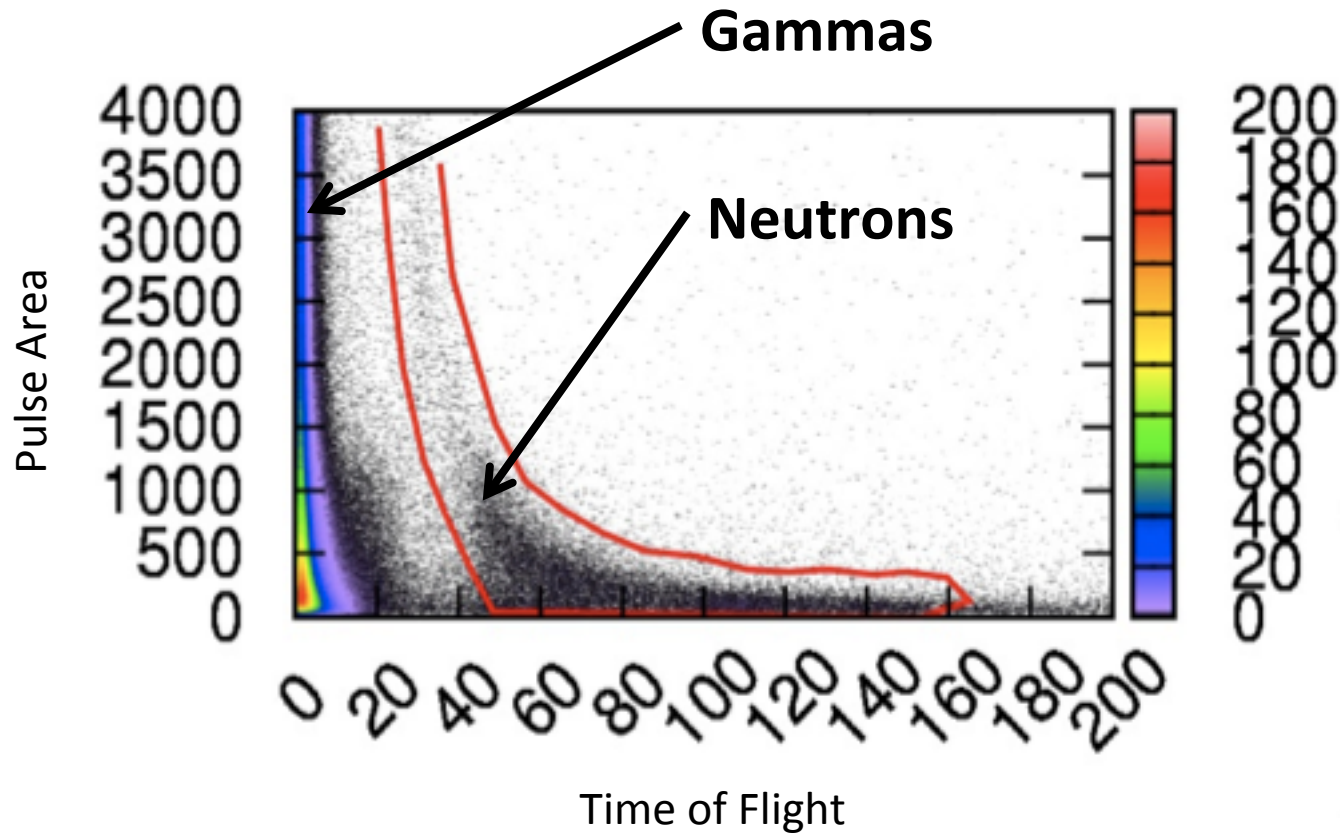
2 Plastic Scintillator β Detectors



Single VANDLE Bar ^{252}Cf Measurements

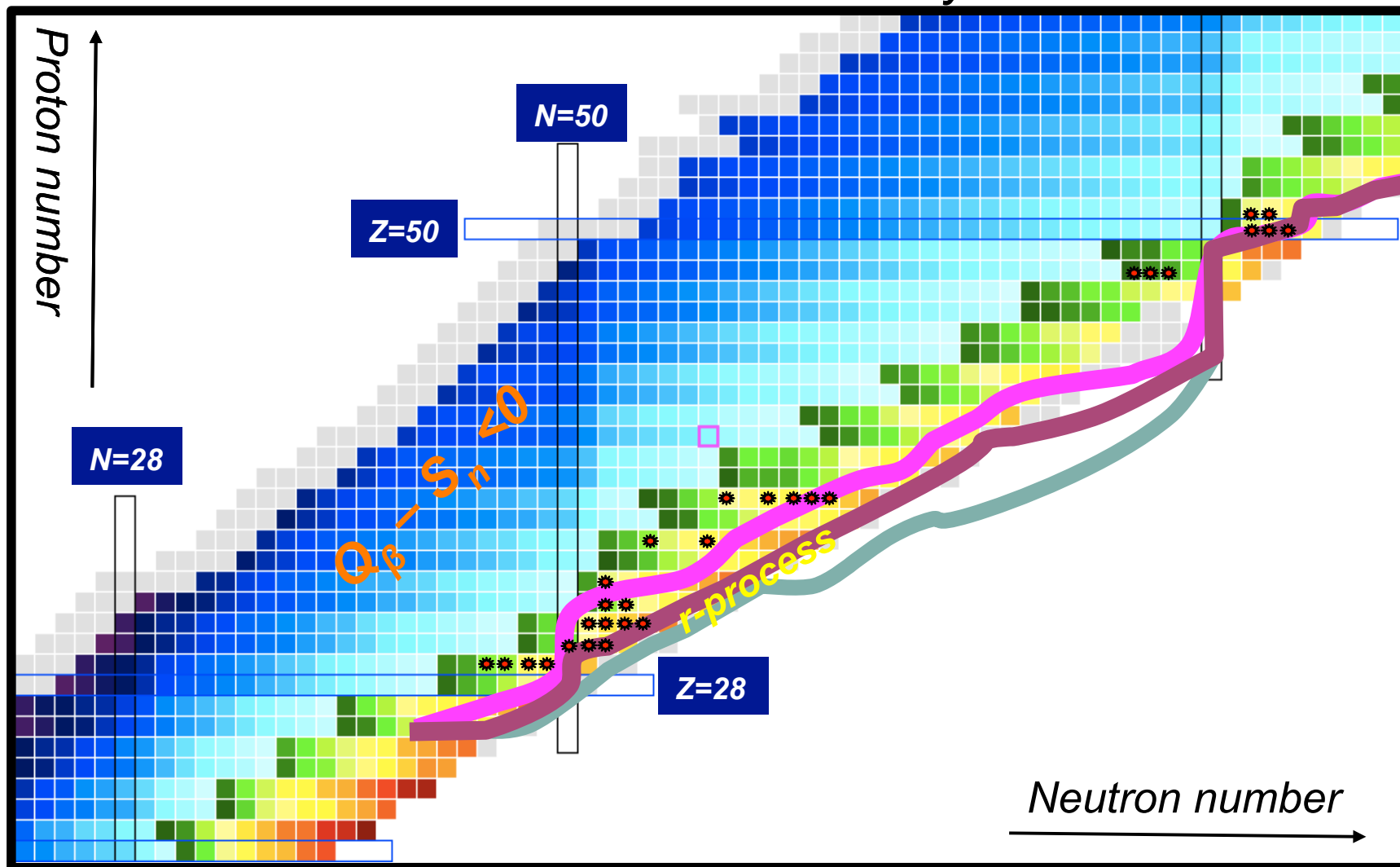


Raw VANDLE Data from ^{77}Cu



The Versatile Array of Neutron Detectors at Low Energy

Beta-delayed neutron emitters near r-process path studied at HRIBF/LeRIBSS in February 2012



VANDLE Collaborators

R. Grzywacz^{1, 2}, S.V. Paulauskas¹, M. Madurga¹, W.A Peters³, C.J. Gross², D.T. Miller¹,
M. Al-Shudifat¹, D.W. Bardayan², J.C. Batchelder³, J. Blackmon⁴, N.T. Brewer⁵, L. Cartegni¹,
K. Chipps⁸, J.A. Cizewski⁶, P.A. Copp⁷, M.E. Howard⁶, S. Ilyushkin⁸, C. Jost², A. Kuzniak⁹, S. Liu³,
B. Manning⁶, C. Matei³, M. Matos⁶, A.J. Mendez II², K. Miernik², P.D. O'Malley⁶, S. Padgett¹,
B.C. Rasco⁴, D. Stracener², F. Raiola⁸, A. Ratkiewicz⁶, K. Rykaczewski², F. Sarazin⁸, K.T. Schmitt²,
I. Spassova³, D. Walter⁶, E.H. Wang⁵, M. Wolinska-Cichocka³, E. Zganjar⁴

¹*Univeristy of Tennessee, Knoxville, TN 37996, USA*

²*Oak Ridge National Laboratory, Oak Ridge, TN 37830, USA*

³*Oak Ridge Associated Universities, Oak Ridge, TN 37831, USA*

⁴*Dept. of Physics and Astronomy, Louisiana State University, Baton Rouge, LA 70803, USA*

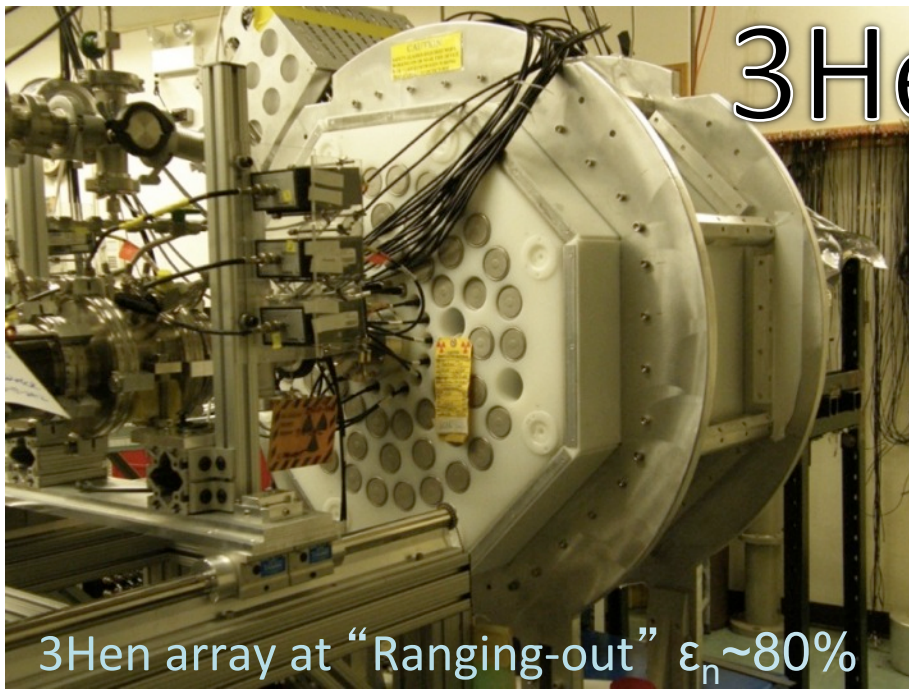
⁵*Vandebilt University, Nashville, TN 37235, USA*

⁶*Rutgers University, Piscataway, NJ 08854-8019 USA*

⁷*University of Wisconsin-La Crosse, La Crosse, WI 54601, USA*

⁸*Colorado School of Mines, Golden, CO 80401, USA*

⁹*University of Warsaw, Warsaw PL-00-681, Poland*



Thermalized Neutron Detector

Hybrid 3Hen Details in ()

74 (48) High Efficiency ^3He Gas Tubes

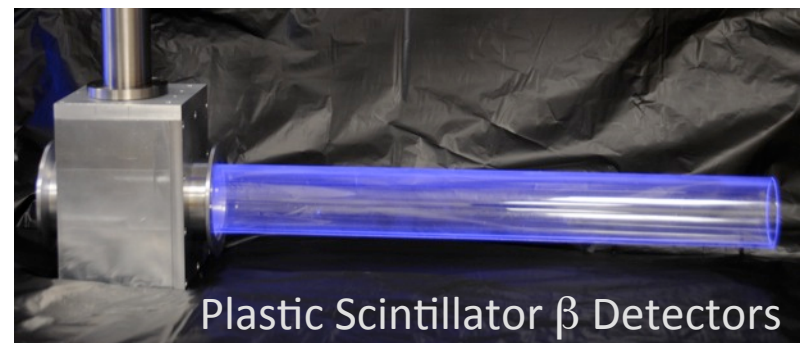
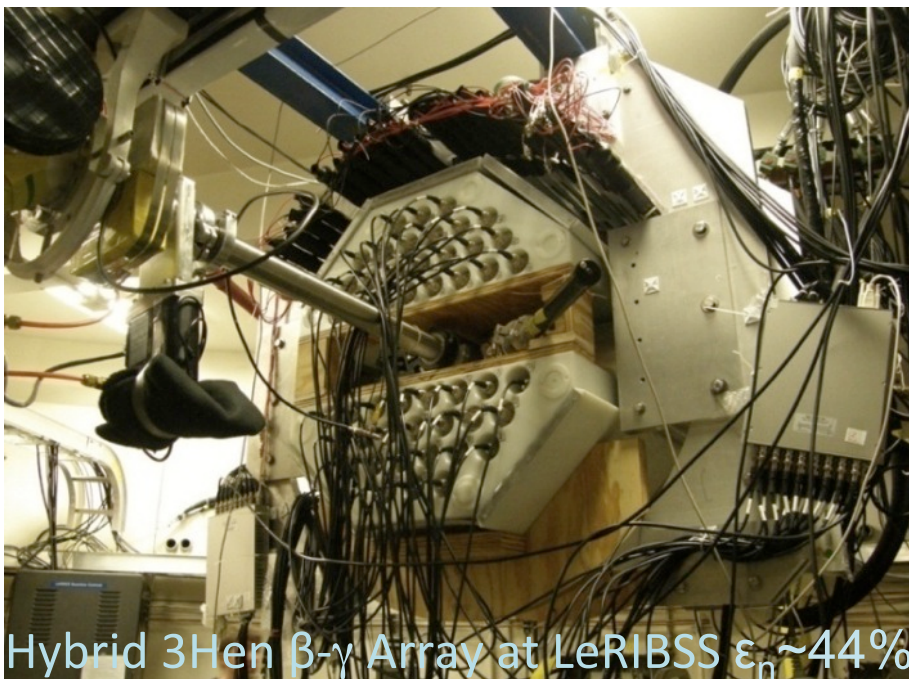
(2 Clover Germanium Detectors)

2 Plastic Scintillator β Detectors

^3He Tubes Surrounded by High Density Polyethylene to Help Thermalize Neutrons

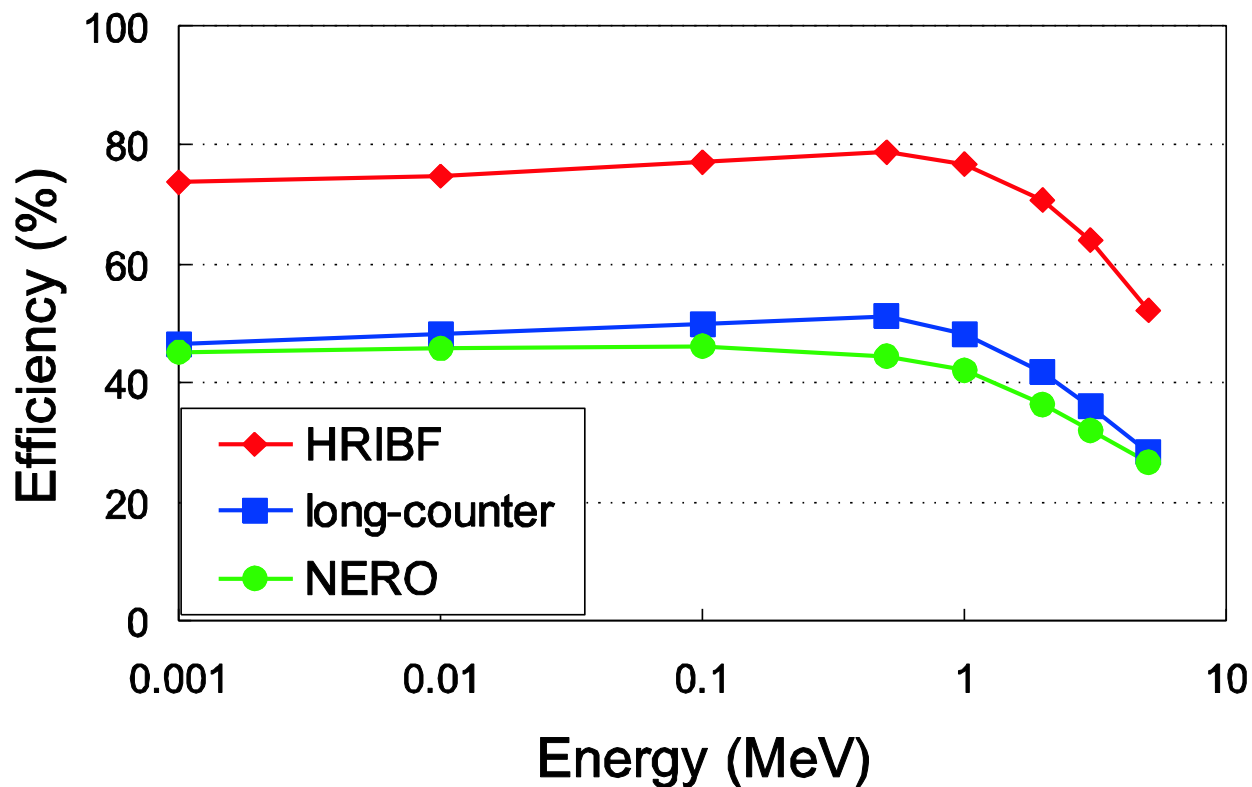
Cadmium Layer Around Edge to Absorb Background Thermal Neutrons

Nuclei Ranged Out in Gas Chamber
(First Experiment with Laser Ion Source
High Purity Exotic ^{86}Ga Delivered)



Comparison of 3He to Other Detectors

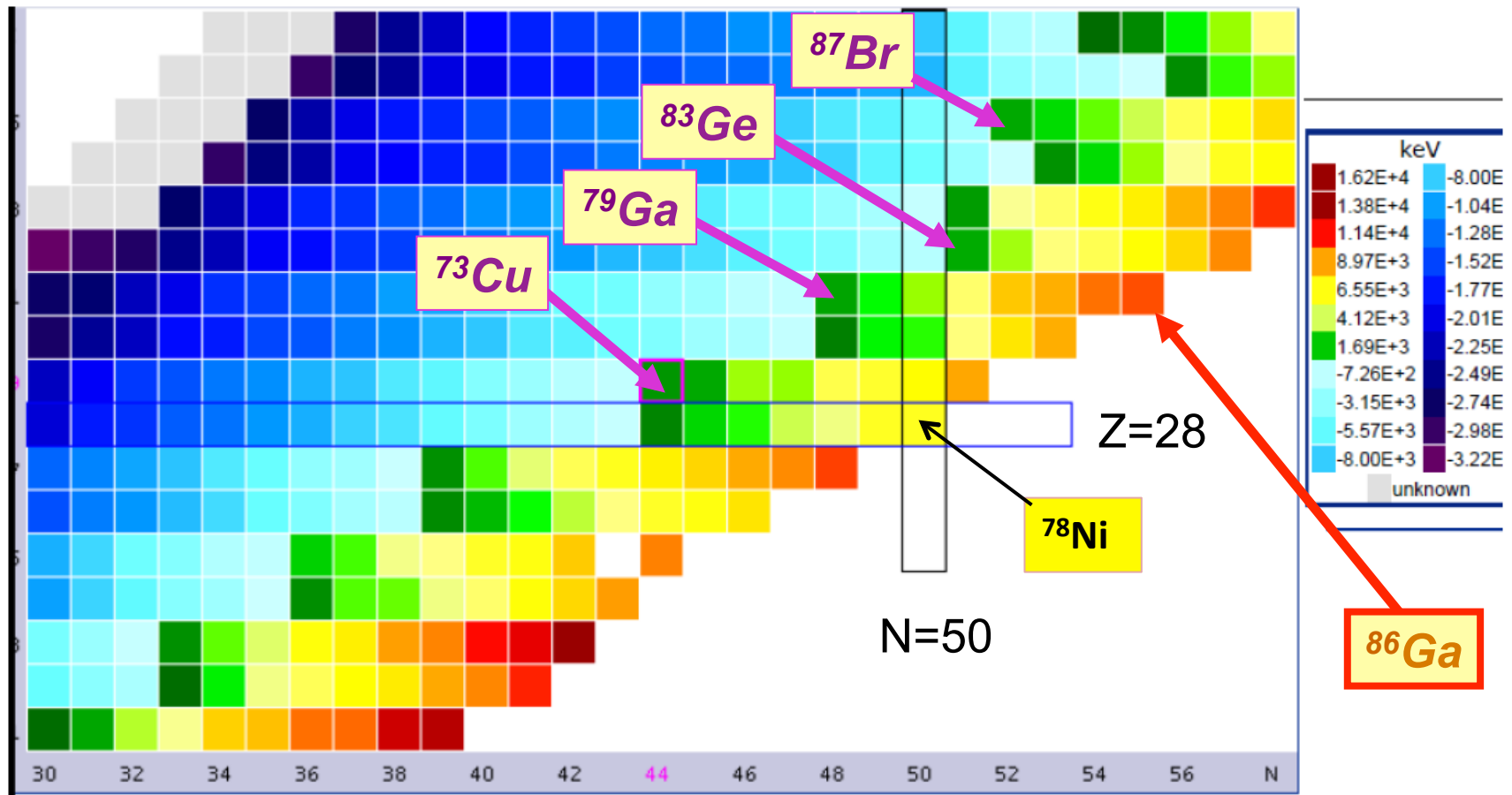
HRIBF, Long-counter, and NERO Neutron Efficiency



Efficiency curve of full 3He detector array (74 3He tubes) compared to the efficiencies of other existing neutron counters like the long-counter of K.L. Kratz and of the NSCL Neutron Observer NERO.

From NNDC :

Energy Window $(Q_\beta - S_n)$ (Q value – Neutron Separation Energy) for β -Delayed Neutron Emission Precursors



Blue – βn emission not possible

Green – $3\text{Hen } I_{\beta n}$ measurements of low energy βn 's

Red-Brown – β -delayed $2n$ emission (low energy?)

3He Collaborators

K.P. Rykaczewski, C.J. Gross, K. Miernik (ORNL Physics Division),
R.K. Grzywacz, K.C. Goetz, M. Madurga, D. Miller, S.V. Paulauskas (UTK),
M. Wolińska-Cichocka (ORAU/ORNL),
I. Gauld (ORNL NST Division),
B.C. Rasco, E. Zganjar (LSU),
J.A. Winger (Mississippi),
A. Fijałkowska, M. Karny, A. Korgul, C. Mazzocchi (University of Warsaw)

Conclusion

Beta decay of neutron rich nuclei is important for understanding nuclear structure, the origins of the elements, and reactor decay heat.

New detector capabilities allow us to study more neutron-rich nuclei with low energy beams

A wealth of new data was acquired at the HRIBF over the last year – now under analysis

Unfortunately the HRIBF has now ceased operations as user facility

ORIC cyclotron being decommissioned

Further Studies using the CARIBU facility at Argonne National Lab and ARIEL at TRIUMF in Canada are Possible

THANK YOU

Backup Slides...

h r i b f

~ 17 μ A proton beam on 6 grams of ^{238}U creates a lot of neutron-rich fission products for spectroscopic studies

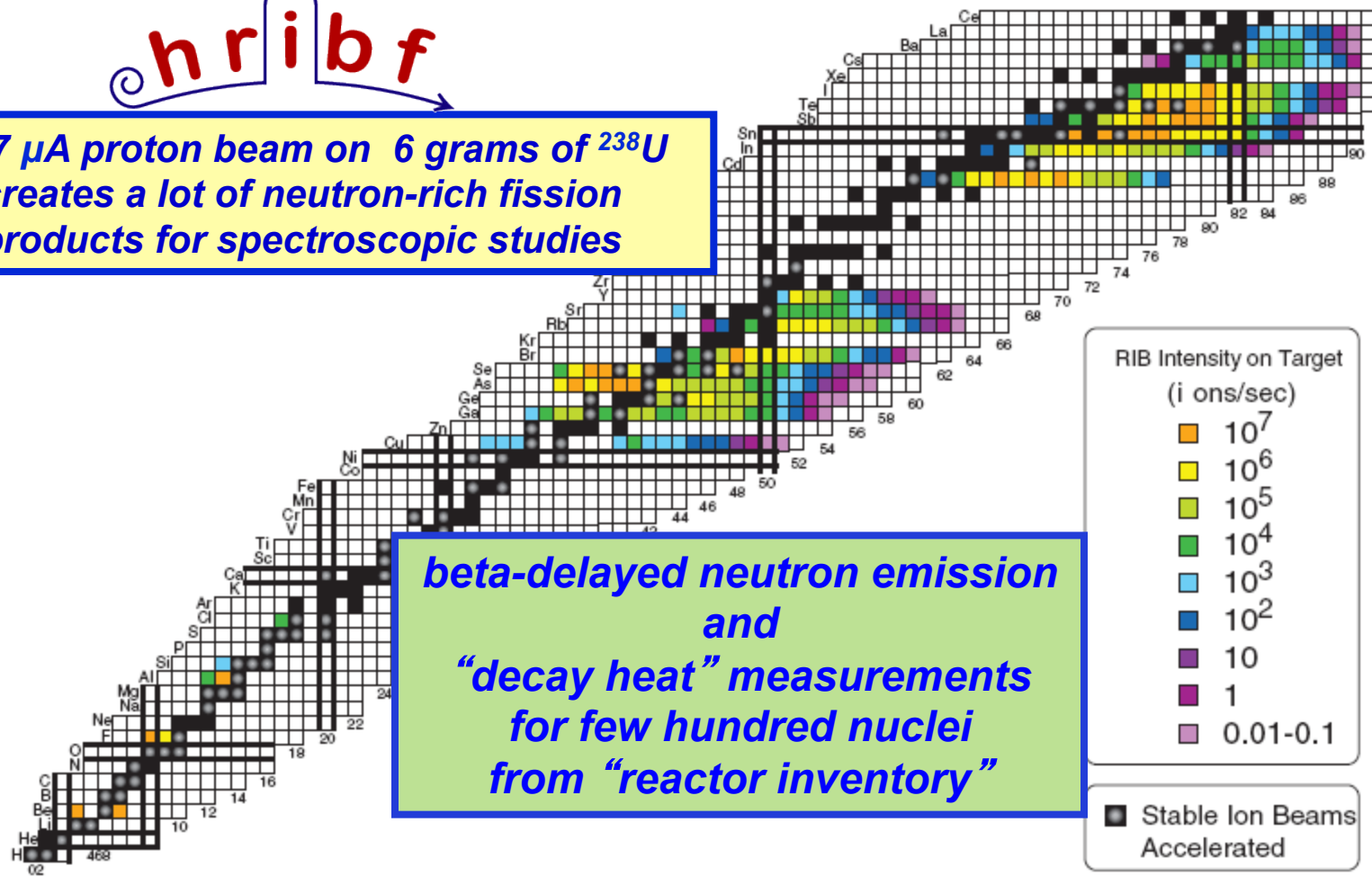
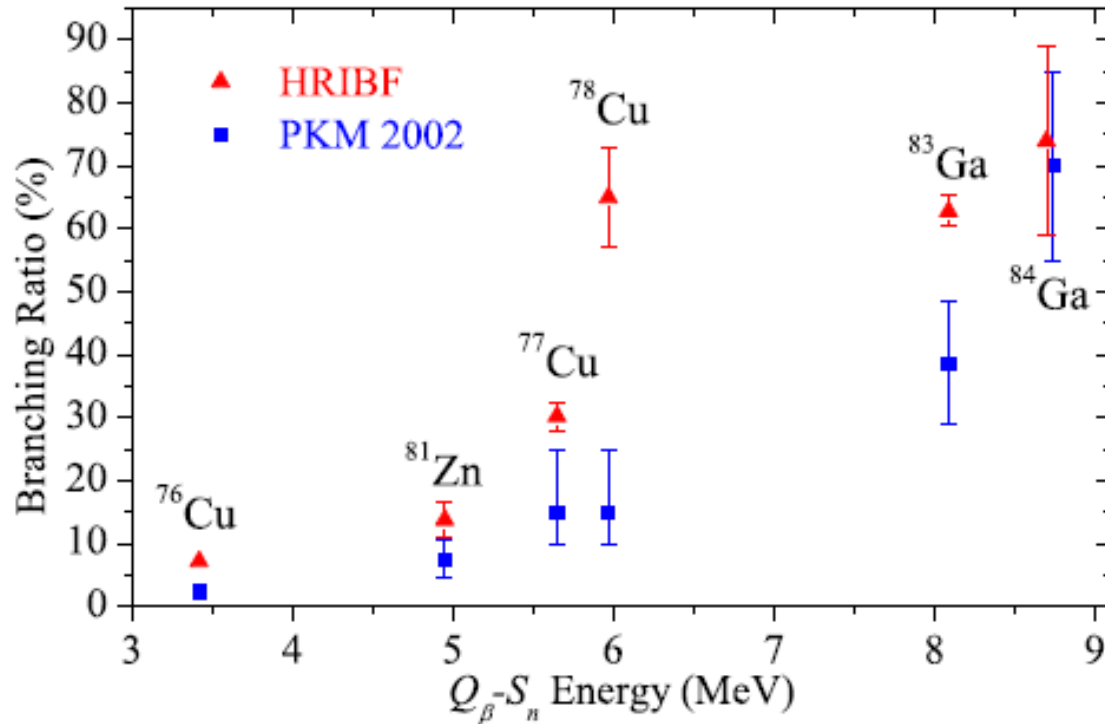


Figure 3. Radioactive and stable beams presently accelerated at the HRIBF. Additional radioactive species such as Zn, Kr, Cd, and Xe are available up to 200 keV as positive ions at LeRIBSS. Stable beams from our new SNICS source [11] are used for RIB development. They are also used to simulate RIBs for tuning and developing new techniques as well as to calibrate detectors.

poster Dan Stracener

Recent HRIBF data

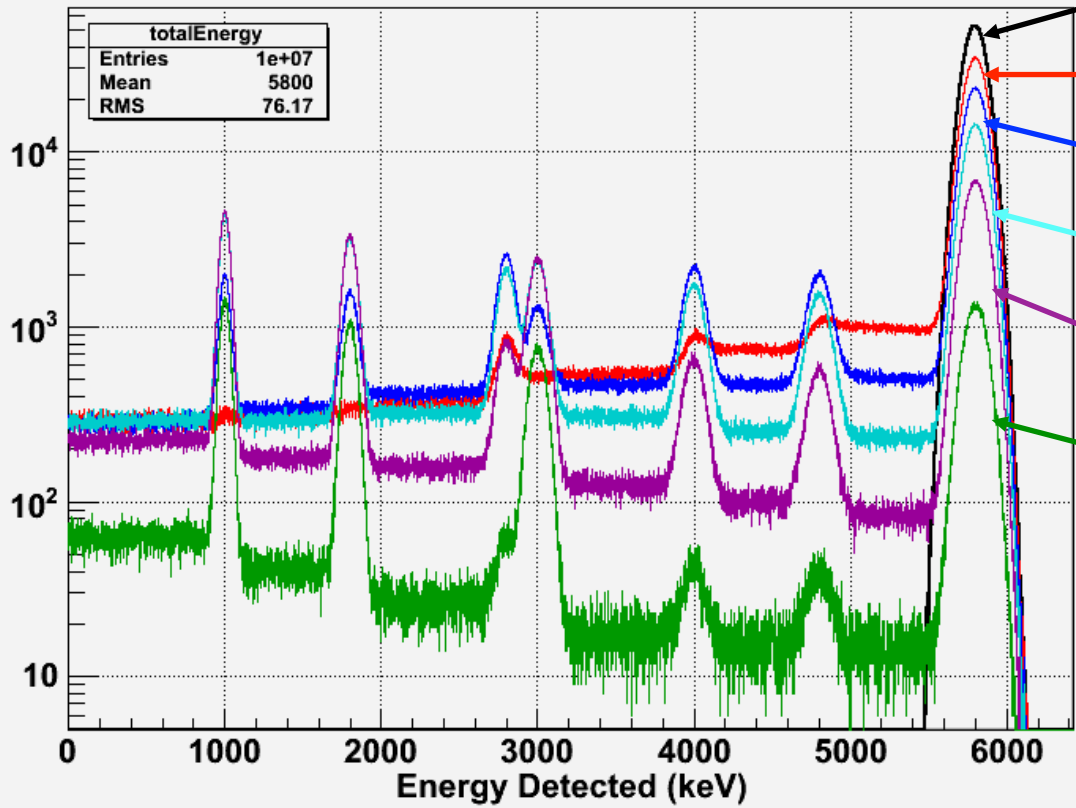
Winger et al., PRL 102, 142501 (2009); PR C 80, 054304 (2009); PR C81, 044303 (2010), PR C82, 064314 (2010), PR C83, 014322 (2011)
are pointing to much higher β n-branching ratios in the ^{78}Ni region
in comparison to earlier measurements and calculations,
see, e.g., **Pfeiffer, Kratz, Moeller (PKM 2002) Prog. Nucl. Energy, 41, 5 (2002)**



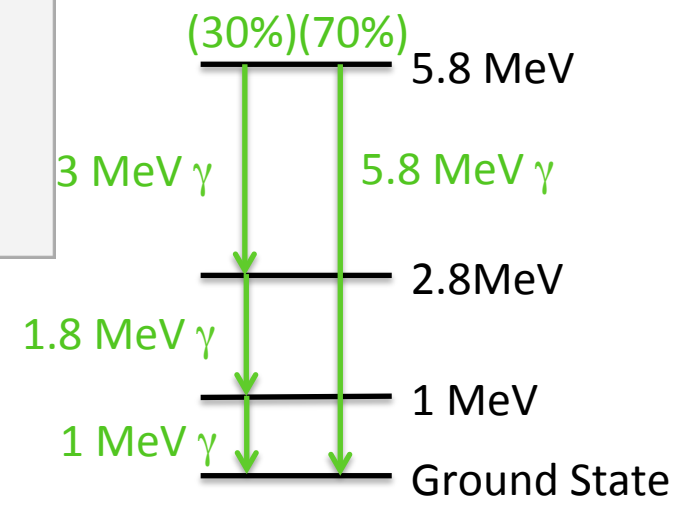
Similar conclusion from a recent NSCL paper basing on NERO results
P. Hosmer, H. Schatz et al., PR C82 , 025806, 2010

**starts to be relevant for
nuclear fuel cycle ?!**

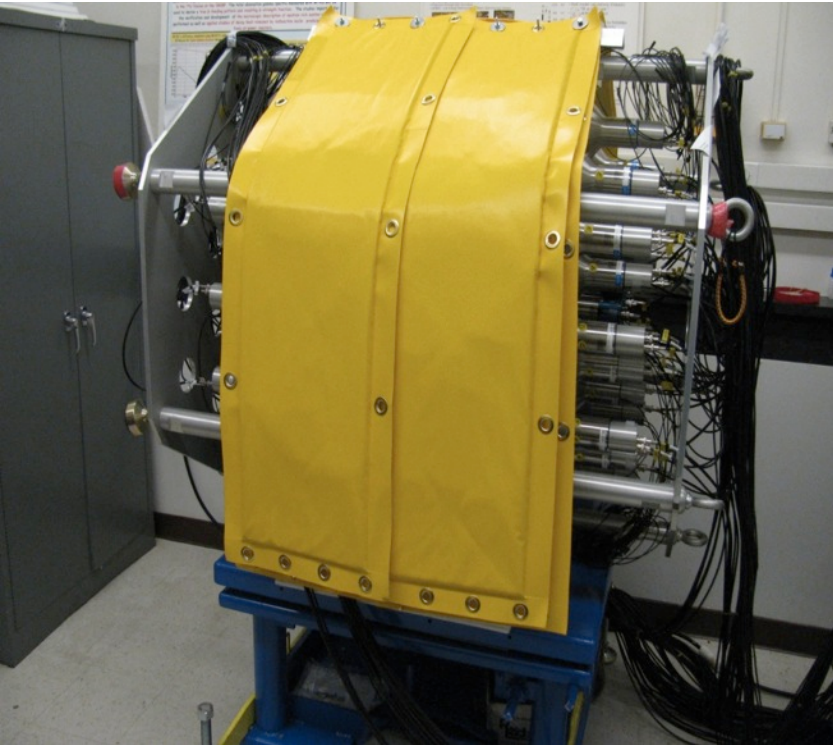
Detected Energy Hypothetical Single Level into 1 γ (.7, 5800keV) or 3 γ s (.3, 1000, 1800, 3000 keV) (100% Efficient-Black, MTAS-Red, 75%MTAS-Blue, 50%MTAS-Cyan, 25%MTAS-Magenta, 5%MTAS-Green)



- 100% Efficient Detector
- MTAS
- 75% Solid Angle Coverage MTAS
- 50% Solid Angle Coverage MTAS
- 25% Solid Angle Coverage MTAS
- 5% Solid Angle Coverage MTAS



MTAS Shielding



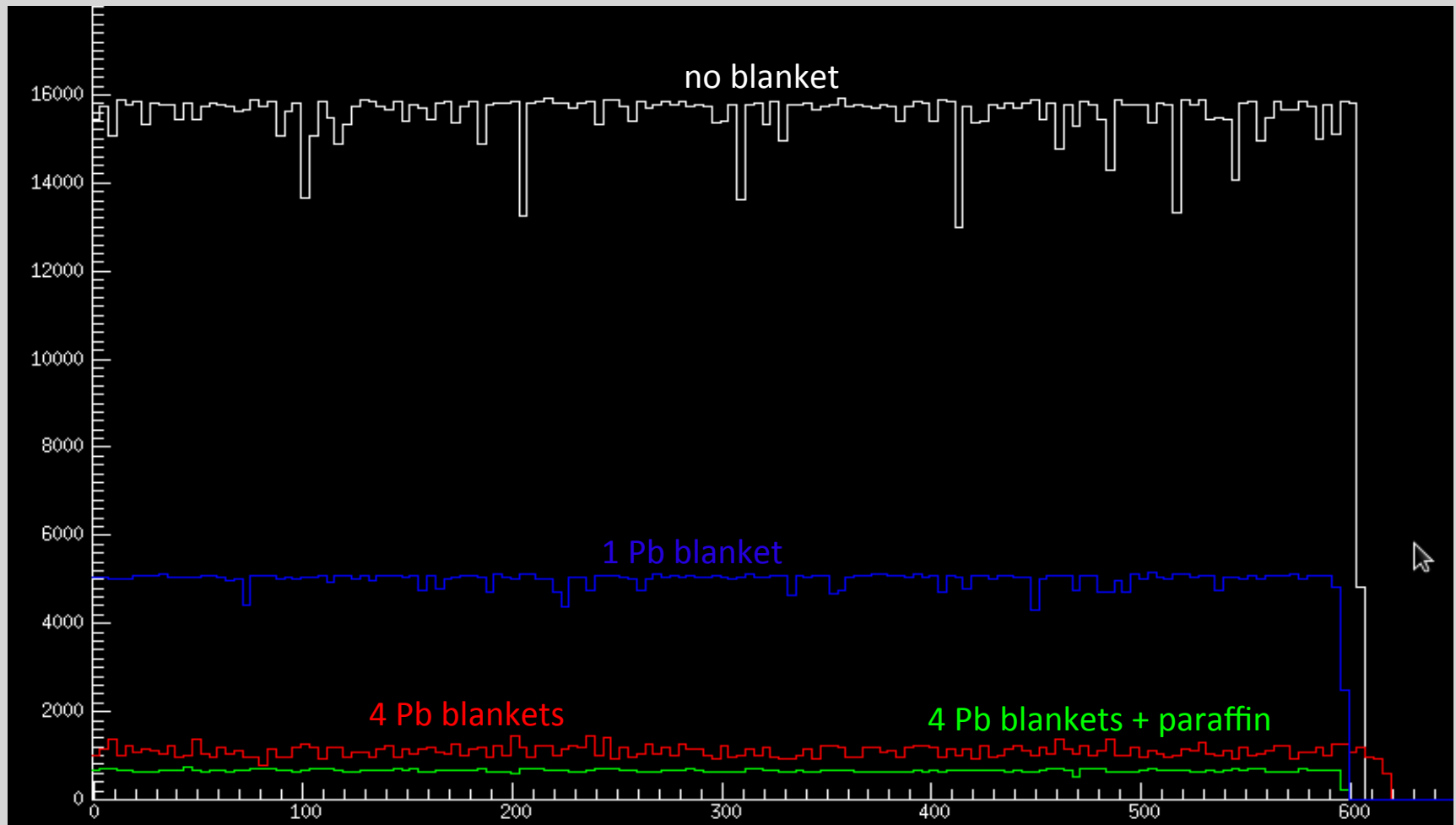
“light” lead shielding
lead wool blankets
~ $\frac{3}{4}$ ” lead equivalent



MTAS test stand was assembled
next to the radioactivity storage room
in order to test data transfer speed

Shielding Tests

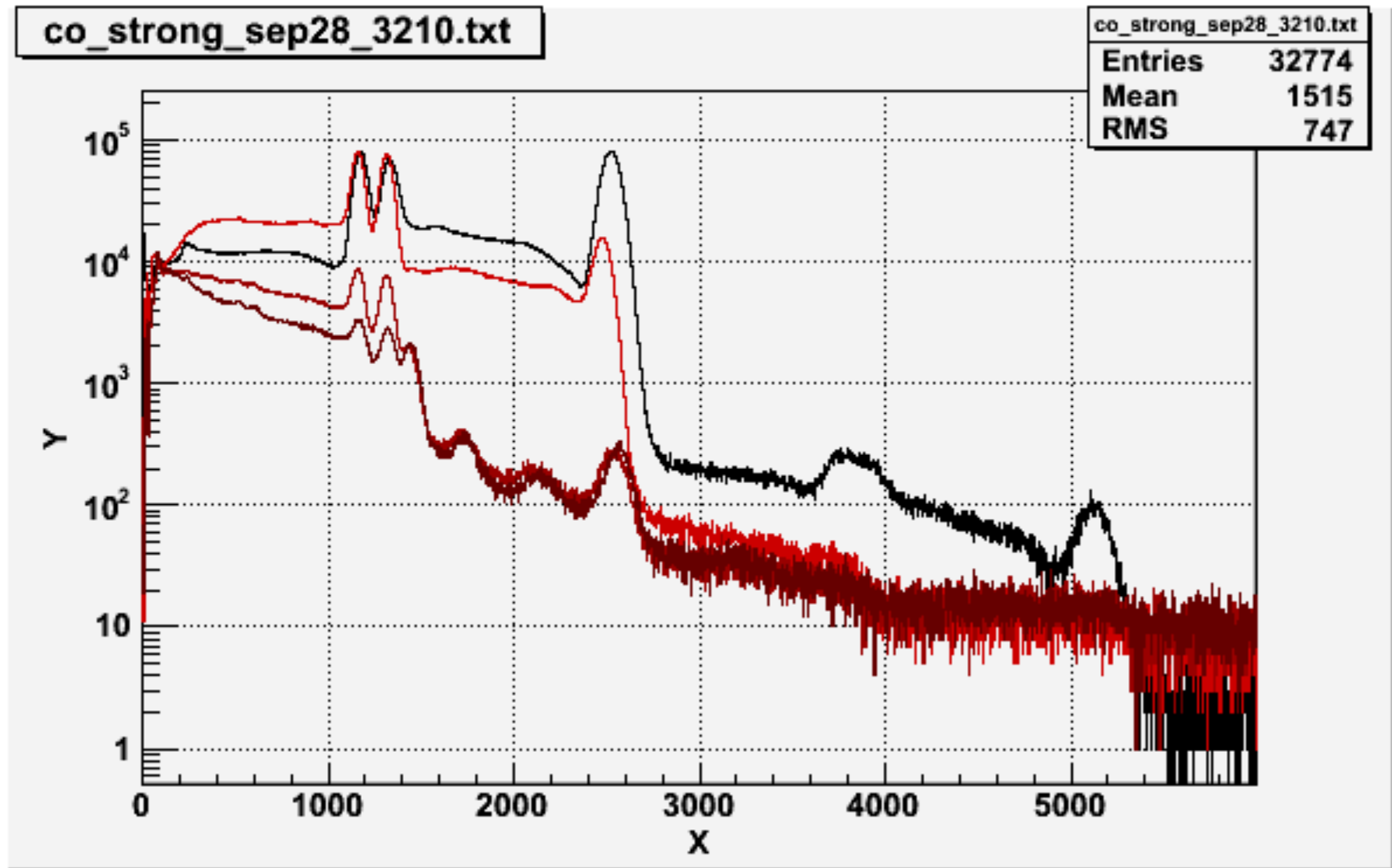
Background level per module went down from ~ 16000 Hz to ~ 600 Hz



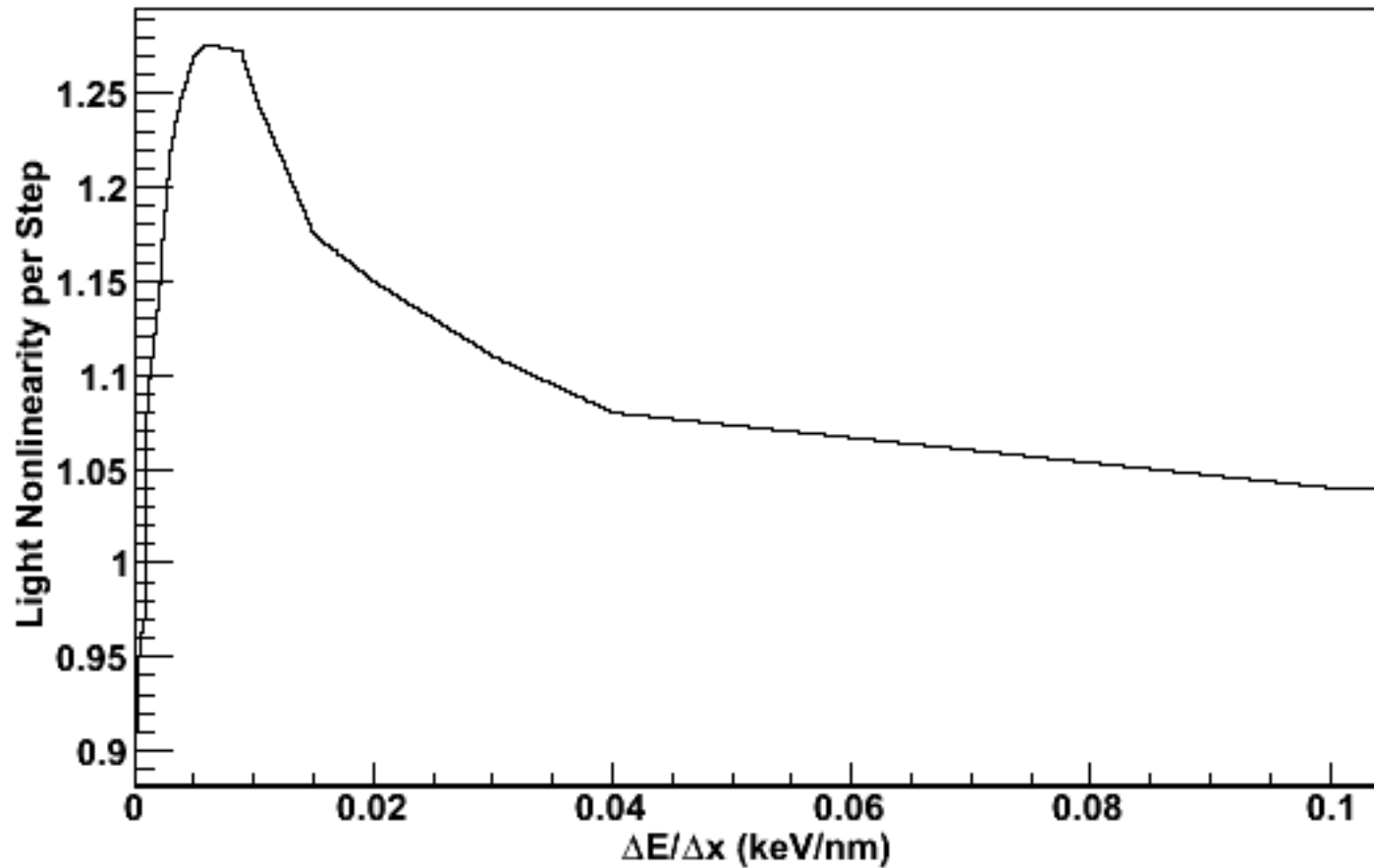
MTAS Tape Drive System



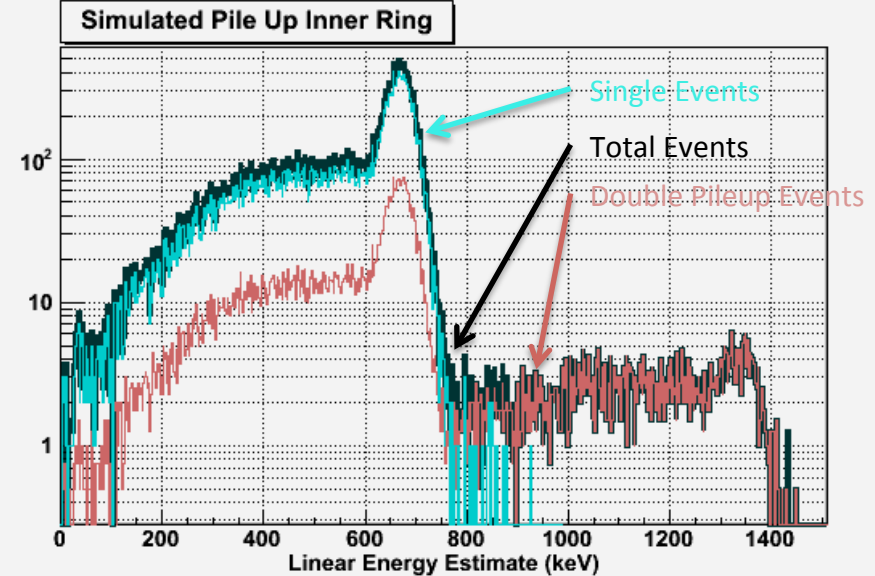
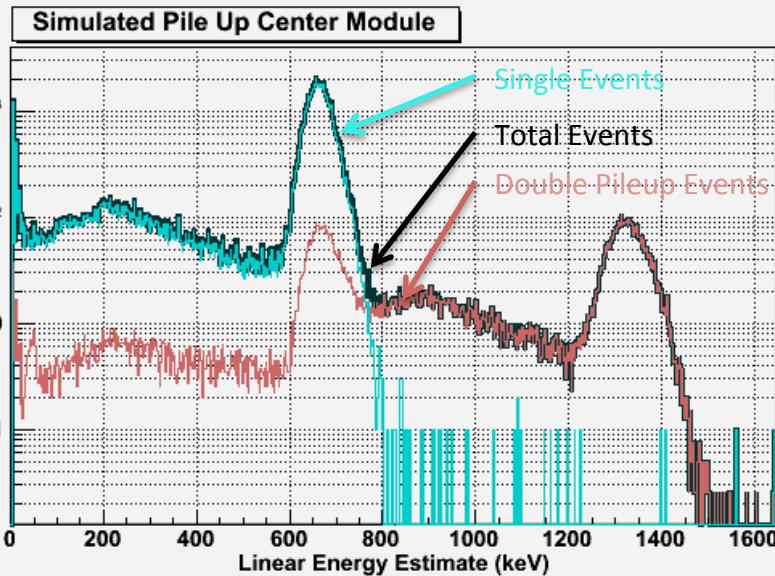
^{60}Co Data By Ring



dE/dx Curve Calculated from and Used in GEANT



Simulation of Light Production in NaI(Tl) Event Pile Up



Simulated pileup of one and two event ¹³⁷Cs
in the central module

Simulated pileup of one and two event ¹³⁷Cs
in the inner ring

The probability for the next event to occur is given by $P(t) = e^{-\lambda t}$ λ -source activity

If this time is less than the digitizer acquisition time then a pileup has happened
(with no event rejection)

For decays with changing activity, which includes most of the planned MTAS experiments,
pileup peak heights will decrease as the activity decreases.

Comparison of relative peak heights versus time distinguishes pile up peaks from real peaks.

^{87}Kr Info

Sr 87 231 h 7.00	Sr 88 82.58	Sr 89 50.5 d	Sr 90 28.64 a	Sr 91 9.5 h	Sr 92 2.71 h	Sr 93 7.45 m
Rb 86 1.02 m 18.7 d	Rb 87 27.835 $4.8 \cdot 10^{10}$ a	Rb 88 17.8 m	Rb 89 15.2 m	Rb 90 4.9 m 2.6 m	Rb 91 58 s	Rb 92 4.5 s
Kr 85 4.48 h 10.76 s	Kr 86 17.3	Kr 87 76.3 m	Kr 88 2.84 h	Kr 89 3.18 m	Kr 90 32.3 s	Kr 91 8.6 s
Br 84 6.0 m 31.8 m	Br 85 2.87 m	Br 86 55.1 s	Br 87 55.7 s	Br 88 16.3 s	Br 89 4.40 s	Br 90 1.9 s
Se 83 89 s 22.4 m	Se 84 3.1 m	Se 85 33 s	Se 86 14.1 s	Se 87 5.8 s	Se 88 1.5 s	Se 89 0.4 s
As 82 14.0 s 19.1 s	As 83 13.3 s	As 84 4.5 s	As 85 2.03 s	As 86 0.9 s	As 87 0.73 s	As 88
Ge 81 7.8 s 7.5 s	Ge 82 4.60 s	Ge 83 1.85 s	Ge 84 984 ms	Ge 85 535 ms	Ge 86	2.540
Ga 80 1.70 s	Ga 81 1.22 s	Ga 82 0.60 s	Ga 83 0.31 s	Ga 84 85 ms		1.327 54 1.963

^{87}Kr β^- Decay 1971Sh01,1973BIZH,1973GeYV

Decay Scheme

Intensities: I(γ +ce) per 100 parent decays

